

IPMU 15-0034
UT-15-08

On skein relations in class S theories

Yuji Tachikawa^{b,‡} and Noriaki Watanabe[‡]

- ^b Department of Physics, Faculty of Science,
University of Tokyo, Bunkyo-ku, Tokyo 133-0022, Japan,
- [‡] Kavli Institute for the Physics and Mathematics of the Universe,
University of Tokyo, Kashiwa, Chiba 277-8583, Japan

Abstract

Loop operators of a class S theory arise from networks on the corresponding Riemann surface, and their operator product expansions are given in terms of the skein relations, that we describe in detail in the case of class S theories of type A. As two applications, we explicitly determine networks corresponding to dyonic loops of $\mathcal{N}=4$ SU(3) super Yang-Mills, and compute the superconformal index of a nontrivial network operator of the T_3 theory.

Contents

1	Introduction and summary	2
2	Loop operators in 4d and skein relations in 2d	4
2.1	Sums and products of loops	4
2.2	Non-commutativity and the angular momentum	6
3	Networks and skein relations in 2d	6
3.1	Generalities	7
3.2	Restriction of labels	8
3.3	Canonical junctions and removal of digons	9
3.4	Crossing resolutions	12
3.5	Reidemeister moves	16
3.6	More simplifying relations	17
3.7	Examples: A_2 and A_3	18
4	Networks for $\mathcal{N}=4$ Yang-Mills	20
4.1	The product of Wilson loops and 't Hooft loops	21
4.2	Analysis in the Liouville/Toda theory	22
4.3	Examples of products of loops in A_2	25
4.4	Classification of networks on T^2 for A_2	28
5	Some examples in the superconformal index	30
5.1	The superconformal indices without lines	31
5.2	4d Wilson Lines	32
5.3	A network in the T_3 theory	33
A	Examples of OPE and charge/network dictionary	36
A.1	Pure dyonic loops	36
A.2	$W_{\square} \times T_{\square}$	37
A.3	$W_{(2,1)} \times T_{\square}$	37
A.4	$W_{\square\Box} \times T_{\square}$	38
A.5	$W_{\text{Adj}} \times T_{\square}$	39
A.6	$W_{\text{Adj}} \times T_{\text{Adj}}$	40
A.7	An OPE of complex dyonic loops	41

1 Introduction and summary

To understand the properties of 4d $\mathcal{N}=2$ supersymmetric theories, it is extremely useful to realize them as twisted compactifications of the 6d $\mathcal{N}=(2,0)$ superconformal field theories (SCFTs) on Riemann surfaces C with punctures [1, 2]. These 4d theories are now called class S theories, and they are closely associated to certain 2d theories defined on C . For example, class S theories on S^4 are related to the Liouville/Toda CFT on C [3, 4] and when considered instead on $S^3 \times S^1$ they give rise to 2d q -deformed Yang-Mills on C [5–7].

How do supersymmetric defects¹ appear under these 4d-2d duality relations? In this paper, we only consider one-dimensional objects, *loops*, on the 4d side. Since 6d $\mathcal{N}=(2,0)$ SCFTs have codimension-two defects and codimension-four defects, a loop operator on the 4d side should come from a codimension-four defect on a codimension-one defect on the 2d side.

For class S theories of type $SU(2)$, or equivalently A_1 , dyonic charges of loops on the 4d side is in one-to-one correspondence with topologies of non-intersecting loops on the 2d side [8]. When the 2d theory is the Liouville/Toda theory, these loops on the 2d side have an explicit realization in terms of the Verlinde operators [9] as shown in [10, 11]. When the 2d theory is the q -deformed Yang-Mills, these loops are instead realized as 2d Wilson loops.²

We only have to consider non-intersecting loops on the Riemann surface for the A_1 case, thanks to the existence of a skein relation resolving each crossing into a sum of two non-crossing ones :

$$\left. \begin{array}{c} \diagup \diagdown \\ \times \end{array} \right) = \mathfrak{q}^{-1/2} \quad \left(+ \mathfrak{q}^{1/2} \begin{array}{c} \diagup \\ \diagdown \end{array} \right. , \quad (1.1)$$

where $\mathfrak{q} = e^{\pi i b^2}$ in the Liouville theory and $\mathfrak{q} = q^{1/2}$ in the q -deformed Yang-Mills.

However, in the higher rank cases, namely for $SU(N)$ with $N > 2$ or equivalently for A_k with $k = N - 1 > 1$, there is no such simple skein relation, since junctions of lines inevitably appear. This results in the networks³ of lines on the Riemann surface, as already mentioned in [12, 13]. Such networks were treated and discussed in [14, 15], putting special emphasis on the $SU(3)$ case. In [14] the analysis was mainly carried out using the approach of the higher Teichmüller theory classically ($\mathfrak{q} = 1$), and in [15] the study was done mainly in the framework of Toda CFTs for general \mathfrak{q} . These analyses gave rise to the skein relations that had been discovered in the context of mathematics before [16].

Our aim in this paper is to describe the skein relations of the networks in the general

¹In this paper we use the words *defects* and *operators* interchangeably.

²This fact was not explicitly mentioned in the literature to the authors' knowledge, but apparently it has been known to many practitioners in the field. We spell this out in Sec. 5.2.

³The same objects are also called as *webs* or *spiders*. In this paper, we only use the terminology *networks*.

$SU(N)$ case. We have, for example, the relation

$$\begin{array}{c} \diagup \quad \diagdown \\ \square \quad \square \end{array} = q^{\frac{1}{N}-1} \begin{array}{c} \uparrow \\ \square \end{array} + q^{\frac{1}{N}} \begin{array}{c} \uparrow \\ \square \end{array} + q^{\frac{1}{N}} \begin{array}{c} \square \\ \diagup \quad \diagdown \\ \square \quad \square \end{array} \quad (1.2)$$

that reduces to the equation (1.1) when $N = 2$. These skein relations were first found in [17] in the context of knot invariants.

The guiding principle for us is that the representation theory of the quantum group $SU_q(N)$ underlies these networks and their skein relations. The relation of the loop operators of 2d CFTs and the quantum group has been known for quite some time, mainly in the context when q is a root of unity, see e.g. [18]. In the case of 2d q -deformed Yang-Mills, the relation of their loops and the quantum group is very direct, because the q -deformed Yang-Mills is a gauge theory whose gauge group is the quantum group [19, 20].

We have two applications of the skein relations. The first concerns the dyonic loop operators of $\mathcal{N}=4$ $SU(N)$ Yang-Mills theory. From the 4d gauge theory perspective, their classification was performed in [21]. When the electric charge and the magnetic charge of a dyonic loop are parallel in the weight system, there is an obvious realization of such dyonic loop in the class S language as a loop wrapping the torus. When they are not parallel, it was expected that they are represented by networks on the torus. We will give a complete description in the case of $SU(3)$.

The second application is the study of a particular loop operator of the T_3 theory. The T_N theory is a strongly-coupled class S theory that does not have a useful Lagrangian description, and there is no direct method to describe a loop operator using the path integral language. Still, using the class S language, it is easy to see that there is a loop operator described by a nontrivial network on a three-punctured sphere. We compute the superconformal index of the T_3 theory in the presence of this loop operator, and confirm that it indeed has an enhanced E_6 symmetry, as expected from the fact [1] that the T_3 theory is in fact the E_6 theory of Minahan and Nemeschansky [22].

The rest of the paper is organized as follows: in Sec. 2, we start by reviewing the relation of the operator product expansion of the loop operators on the 4d side and the skein relation on the 2d side. We emphasize the universality of the skein relation, independent of the choice of the 4d spacetime. Next, in Sec. 3, we describe the skein relations explicitly for general $SU(N)$. We also explain how they can be understood in terms of the representation theory of quantum groups. In Sec. 4, we turn to an application on 4d $\mathcal{N}=4$ gauge theory. We discuss the operator product expansion of a pure Wilson loop and a pure 't Hooft loop in the general $SU(N)$ theory. We also describe all the dyonic loops in the $SU(3)$ theory in terms of networks, and point out a relation to the brane tiling. In Sec. 5, we first explain how the 4d Wilson loop is mapped to the 2d Wilson loop in the context of the q -deformed Yang-Mills. We then use one of the skein relations to compute the superconformal index of the T_3 theory in the presence of a loop operator

corresponding to the simplest nontrivial network. In the Appendix A, we have more examples of the realization of dyonic loops by networks in the general $SU(N)$ theory.

2 Loop operators in 4d and skein relations in 2d

In the Liouville theory, a Verlinde loop operator is defined in terms of monodromy actions on the conformal block \mathcal{F} along a loop γ . It is possible to insert more than one Verlinde operator and $\mathcal{L}_{\gamma_A} \mathcal{L}_{\gamma_B} \mathcal{F} \neq \mathcal{L}_{\gamma_B} \mathcal{L}_{\gamma_A} \mathcal{F}$ in general when γ_A and γ_B intersect each other, as we see from the concrete calculations. See Fig. 1 for an illustration.

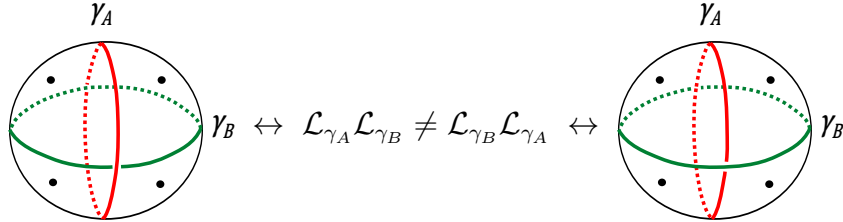


Figure 1: Non-commutativity of actions of loop operators.

Under the 2d-4d correspondence, the Verlinde operators map to loop operators of the 4d theory. Therefore, there should be a concept of ordering of loops on the 4d side, such that the product becomes non-commutative. In this section we review how this ordering arises, following [23–26]. See also the recent reviews [27, 28].

2.1 Sums and products of loops

We consider the 4d setups where some kind of localization computations is possible. Typically there is a supercharge preserved in the background, whose square involves a linear combination of two isometries $k_{1,2}$. Supersymmetric loops wrap along the direction of k_1 and sit at the fixed point of k_2 .

In the neighborhood of the loop, we can approximate the geometry as $S^1 \times \mathbb{C} \times \mathbb{R}$, where k_1 shifts the coordinate along S^1 and k_2 is the phase rotation of \mathbb{C} . The loop now wraps S^1 and sits at the origin of \mathbb{C} , and the position $x \in \mathbb{R}$ is arbitrary. Therefore, we can place multiple loops $L_{1,2,\dots}$ on $x_{1,2,\dots}$ preserving the same supercharge.

This gives an intrinsic ordering of loops on the 4d side, and furthermore, the expectation values are unchanged under infinitesimal changes of the positions x_i . The choice of the local supersymmetric background at a loop can be characterized by a single parameter which we denote by \mathfrak{q} . These statements can be explicitly checked in the case of the localizations on $S^1 \times S^3$ [12], $S^1 \times \mathbb{R}^3$ [26] and S_b^4 [29].

Given two types of loop defects L_1 and L_2 , we denote loops placed at $x \in \mathbb{R}$ by $L_i(x)$. We define a formal sum $L_1 + L_2$ of two loops by

$$\langle \cdots (L_1 + L_2)(x) \rangle := \langle \cdots L_1(x) \rangle + \langle \cdots L_2(x) \rangle \quad (2.1)$$

where the ellipses stand for other operator insertions. The product $L_1 \cdot L_2$ of two loops are now defined by

$$\langle \cdots (L_1 \cdot L_2)(x) \rangle := \langle \cdots L_1(x_1) L_2(x_2) \rangle \quad (2.2)$$

where we demand $x_1 > x > x_2$ so that L_1 and L_2 are the loops closest to x from the left and from the right. Since the expectation values depend only on the order but independent of the relative distance, this gives a consistent definition.

At this stage, we can make sense of the operator product expansion for defects. Suppose that there is a set $L_{1,2,\dots}$ of loops which cannot be decomposed into any sum of other simpler ones. We then have the following expansion of correlation functions

$$\langle \cdots L_i \cdot L_j(x) \rangle = \sum_k c_{ij}^k(\mathbf{q}) \langle \cdots L_k(x) \rangle \quad (2.3)$$

that can be written succinctly as

$$L_i \cdot L_j = \sum_k c_{ij}^k(\mathbf{q}) L_k. \quad (2.4)$$

The OPE coefficients $c_{ij}^k(\mathbf{q})$ are asymmetric under the exchange $i \leftrightarrow j$ due to the intrinsic ordering along \mathbb{R} . However, we can simultaneously flip the \mathbb{R} direction and S^1 direction in the local $S^1 \times \mathbb{C} \times \mathbb{R}$ geometry to obtain another supersymmetric background. The background is parameterized by \mathbf{q} as remarked before, and we use the parameterization such that this flip is represented by $\mathbf{q} \mapsto \mathbf{q}^{-1}$. Then we should have the relation

$$c_{ij}^k(\mathbf{q}) = c_{ji}^k(\mathbf{q}^{-1}). \quad (2.5)$$

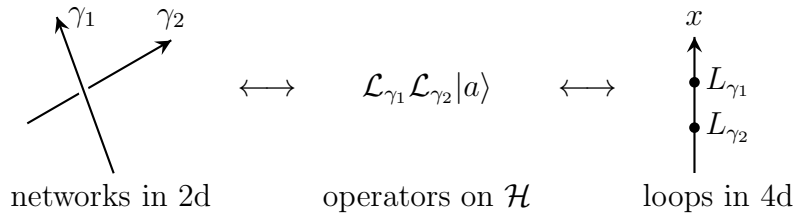


Figure 2: Left: the part of networks γ_1 and γ_2 . For any other crossing of $\gamma_{1,2}$, γ_1 is always above γ_2 . Middle: the expressions acting on $\mathcal{H} = \mathcal{H}_{\text{conf}} = \mathcal{H}_{\text{hemi}}$. Right: the ordering on the 4d side, along \mathbb{R} .

There is also an order for the defect networks on the two dimensional geometry side. In order to make the relation between two orders, let us consider the case when the 4d side is S_b^4 and the 2d side is the Liouville/Toda theory [3, 4]. In this case the Verlinde operators associated to the networks on the 2d side act on the space $\mathcal{H}_{\text{conf}}$ of conformal blocks, and the loop operators on the 4d side act on the space $\mathcal{H}_{\text{hemi}}$ of holomorphic

Nekrasov partition functions defined on a hemisphere [10, 11, 15, 30]. Since $\mathcal{H}_{\text{conf}}$ and $\mathcal{H}_{\text{hemi}}$ are naturally isomorphic, we can see the relations among three orderings as shown in Fig. 2.

Corresponding to (2.4), there should be the operator product expansions of defect networks which are indeed skein relations as resolutions of the crossings. In Sec. 4, we will see that we can calculate many OPE coefficients in terms of defect networks.

2.2 Non-commutativity and the angular momentum

Let us recall the origin of the non-commutativity when the geometry is globally $S^1 \times \mathbb{C} \times \mathbb{R}$, following the discussions in [24, 26]. Considering the S^1 as the time direction, the partition function of $S^1 \times \mathbb{C} \times \mathbb{R}$ is given by

$$\Omega = \text{Tr}_{\mathcal{H}} [(-1)^F e^{2\pi i \lambda \mathcal{J}_3}] \quad (2.6)$$

where \mathcal{H} is the Hilbert space of the system, $\mathcal{J}_3 = J_3 + I_3$ is the sum of the spin along \mathbb{R} and the Cartan of the $\text{SU}(2)$ R-symmetry. Our parameter \mathfrak{q} is then given by $\mathfrak{q} = e^{\pi i \lambda}$.

Suppose now that we have a $\text{U}(1)$ gauge theory, that the first loop L_1 is purely electrically charged with electric charge e and that the second loop L_2 is purely magnetically charged with magnetic charge m . Then there appears the Poynting vector carrying the angular momentum $J_P = (\hbar/2)em$ along the \mathbb{R} direction. The magnitude of J_P is independent of the distance between two particles but the sign depends on the ordering, and therefore we have

$$L_1 \cdot L_2 = \mathfrak{q}^{-2em} L_2 \cdot L_1. \quad (2.7)$$

In the classical limit ($\mathfrak{q} \rightarrow 1$), this product becomes commutative.

3 Networks and skein relations in 2d

In this section we discuss possible types of networks in class S theories of type $\text{SU}(N)$ and their skein relations. Our guiding principle is that they are described by the structure of the quantum groups underlying both the q -deformed Yang-Mills and the Liouville/Toda CFT, and that the skein relations are universal under an appropriate parameter identification. The skein relations exhibited below already appear in the mathematical works [17, 31, 32], up to the overall factors and the changes in conventions.

Skein relations introduce equivalence relations among all possible networks, and it would be extremely useful if we can pick a natural representative element out of a given equivalence class of networks allowing linear combinations of networks. In this paper we at least give a general method to simplify a given network:

- In principle, edges in a network can carry arbitrary representations of $\text{SU}(N)$. We will first rewrite them in terms of representations $\wedge^k \square$ for $k = 1, \dots, N-1$. These

are the fundamental representations in the mathematical terminology,⁴ and within the diagrams we just denote them by $1, 2, \dots, N - 1$.

- Then we rewrite all crossings in terms of linear combinations of junctions that are at most rectangular. The concrete formulas are given in (3.36). We call this process *crossing resolutions*.

In the A_1 case, these procedures eliminate all the crossings and no junctions remain, thus reproducing the classification in [8]. In the A_2 case, we will see that all digons and rectangles can be eliminated, and we will find a natural representative for a given equivalence class of networks. We will detail this process in Sec. 4.4.

Hereafter we use a version of the standard quantum number defined as

$$\langle n \rangle := (-1)^{n-1}[n] := (-1)^{n-1} \frac{q^n - q^{-n}}{q - q^{-1}} \quad (3.1)$$

and the factorial defined as

$$\langle 0 \rangle! = 1, \quad \langle n \rangle! = \langle n \rangle \langle n-1 \rangle!. \quad (3.2)$$

As this section is rather long, let us pause here to explain the organization: in Sec. 3.1, we start by recalling that codimension-4 operators of the 6d $\mathcal{N}=(2,0)$ theory are labeled by representations and they can have junctions corresponding to the invariant tensors. In Sec. 3.2, we describe how an arbitrary representation can be rewritten in terms of just the fundamental representations of the form $\wedge^k \square$. In Sec. 3.3, we then describe the trivalent junctions where three edges labeled by fundamental representations meet. In Sec. 3.4, we show how a crossing of two edges can be rewritten in terms of junctions. We start from the crossing of two edges labeled by \square and then describe the general case. In Sec. 3.5 we summarize the Reidemeister moves that are fundamental equivalence relations guaranteeing the isotopy invariance. In Sec. 3.6 we note other useful skein relations that can be used to simplify networks. Finally in Sec. 3.7, we explicitly display the skein relations for A_2 and A_3 .

In general, it would also be important in the class S theory to study skein relations with full and other punctures in [1] or networks ending on other punctures. We do not, however, consider such objects in this paper.

3.1 Generalities

Before proceeding, let us first recall the fact that a codimension-4 operator of the 6d $\mathcal{N}=(2,0)$ theory of type $SU(N)$ has a label given by a representation of $SU(N)$, and how a multiple number of such operators can be joined.

A cylinder of the $\mathcal{N}=(2,0)$ theory gives rise to a 4d $\mathcal{N}=2$ vector multiplet with gauge group $SU(N)$. On the 4d side, then, we can consider the Wilson loop operator in a

⁴Contrary to the standard physics usage, we do not restrict the fundamental representation to be the defining N -dimensional representation in this paper.

representation R of $SU(N)$. This should come from some codimension-4 operator of the $\mathcal{N}=(2,0)$ theory wrapped around the cylinder. Then this codimension-4 operator also needs to be labeled by a representation R .

When we multiply two parallel Wilson loops with representations R_1 and R_2 , we get a Wilson loop with representation $R_1 \otimes R_2$, and the product is commutative. The same should be then true among codimension-4 operators of the $\mathcal{N}=(2,0)$ theory.

On the 4d side, three Wilson loops in representations $R_{1,2,3}$ can be joined at a point consistently if $R_1 \otimes R_2 \otimes R_3$ contains an $SU(N)$ invariant subspace, or equivalently when there is an invariant tensor in this triple tensor product. The number of independent ways to join them is given by the number of linearly independent invariant tensors. Then, three codimension-4 operators of the $\mathcal{N}=(2,0)$ theory labeled by $R_{1,2,3}$ can be joined along a one-dimensional subspace when there are invariant tensors in $R_1 \otimes R_2 \otimes R_3$. The number of distinct ways to connect is given by the number of linearly independent invariant tensors.

Since this should be an intrinsic property of codimension-4 operators of the 6d theory, we can join three codimension-4 operators along a one-dimensional loop on the 4d side. This gives a junction of three edges labeled by R_1 , R_2 , R_3 on the 2d side. Using many such junctions, we end up having networks on the 2d side, which are our main interest in this paper.

3.2 Restriction of labels

First, note that Wilson loop on the 4d side in a representation R in a direction can be thought of as a Wilson loop in the representation \bar{R} in the opposite direction. This feature should also be carried over to the codimension-4 defects of the $\mathcal{N}=(2,0)$ theory, and to the networks on the 2d side. This can be represented diagrammatically as

$$\longrightarrow R = R^* \longleftarrow . \quad (3.3)$$

As it is cumbersome to use arbitrary representations R as labels, we next rewrite them in terms of fundamental representations $\wedge^k \square$, $k = 1, \dots, N-1$. An irreducible representation R can be specified by a Young diagram (ℓ_i) where ℓ_i is the number of boxes in the i -th row, so that $\sum \ell_i = N$. For example, $\wedge^k \square$ is represented by $(\underbrace{1 1 1 \dots 1}_k) = (1^k)$.

Note that any symmetric polynomial of N variables x_1, x_2, \dots, x_N , under a constraint $x_1 x_2 \dots x_N = 1$, can be written as a polynomial of the elementary symmetric polynomials. As a character $\chi_R(\text{diag}(x_1, \dots, x_N))$ of $SU(N)$ in a representation R is such a symmetric polynomial, and $\chi_{(1^k)}(\text{diag}(x_1, \dots, x_N))$ for $k = 0, 1, 2, \dots, N-1$ are exactly elementary symmetric polynomials, this means that any representation R can be decomposed as the direct sum (allowing negative integral coefficients) of the tensor products of $\wedge^k \square$.

For example, we have the equalities

$$\chi_{(2)} = \chi_{(1)}^2 - \chi_{(1^2)}, \quad \chi_{(21)} = \chi_{(1^2)} \chi_{(1)} - \chi_{(1^3)}, \quad (3.4)$$

$$\chi_{(3)} = \chi_{(1)}^3 - 2\chi_{(1^2)} \chi_{(1)} + \chi_{(1^3)}, \quad \chi_{(2^2)} = \chi_{(1^2)} \chi_{(1^2)} - \chi_{(1)} \chi_{(1^3)} \quad (3.5)$$

which we can diagrammatically depict, in the case of closed loops, as

$$\begin{array}{c} \text{Diagram 1: } \text{Diagram 2} = \text{Diagram 3} - \text{Diagram 4}, \\ \text{Diagram 2: } \text{Diagram 5} = \text{Diagram 6} - \text{Diagram 7}, \end{array} \quad (3.6)$$

$$\begin{array}{c} \text{Diagram 8: } \text{Diagram 9} = \text{Diagram 10} - \text{Diagram 11}, \\ \text{Diagram 10: } \text{Diagram 12} = \text{Diagram 13} - 2 \text{Diagram 14} + \text{Diagram 15}. \end{array} \quad (3.7)$$

These relations are locally applicable on parallel edges. Therefore, we can insert some punctures or networks inside the circle, for example.

3.3 Canonical junctions and removal of digons

3.3.1 Canonical junctions

Now our edges are labeled by the fundamental representations $\wedge^k \square$, $k = 0, 1, \dots, N - 1$. We can just use the integer k to label the edge, and an edge labeled by 0 can be removed. Reversing the orientation now corresponds to replacing the label k by $N - k$. An edge labeled by k has charge k under the center of $SU(N)$, and therefore we call these integer labels as the *charge*.⁵

For each trivalent junction, the sum of three inflowing charges must equal to zero modulo N . Say we have three edges labeled by a , b and $c = a + b$. There is only a single invariant tensor in $\wedge^a \square \otimes \wedge^b \square \otimes \wedge^{N-c} \square$, and this corresponds to the projection from $\wedge^a \square \otimes \wedge^b \square$ to $\wedge^{c=a+b} \square$. Therefore, there is no need to place a label on a junction to distinguish the possible invariant tensors.

Sometimes these labels k are then taken to be defined modulo N as in [14, 15], but it is useful to consider them just as integers between 0 and $N - 1$. This is because we can write down the invariant tensor rather explicitly using the quantum group representation theory when the net inflowing charge to a junction vanishes in \mathbb{Z} . We call such a junction *canonical*. We call a junction non-canonical if the net inflowing charge vanishes only in \mathbb{Z}_N . See Fig. 3 for examples.

Let us now describe the invariant tensors associated to the canonical junctions. Let \square be spanned by the vectors e_1, \dots, e_N . We define the q -deformed wedge product by the rule

$$e_i \wedge e_j = -q e_j \wedge e_i, \quad (i \leq j) \quad (3.8)$$

where in particular $e_i \wedge e_i = 0$ where we do not sum over i . This defines the projection π from $\square \otimes \square$ to $\wedge^2 \square$ by

$$\pi_{1,1 \rightarrow 2} : e_i \otimes e_j \mapsto e_i \wedge e_j. \quad (3.9)$$

⁵Note that it is a special property of A_k that there is the one-to-one correspondence of the set of the fundamental representations $\wedge^k \square$ including the trivial one and the charge under the center.

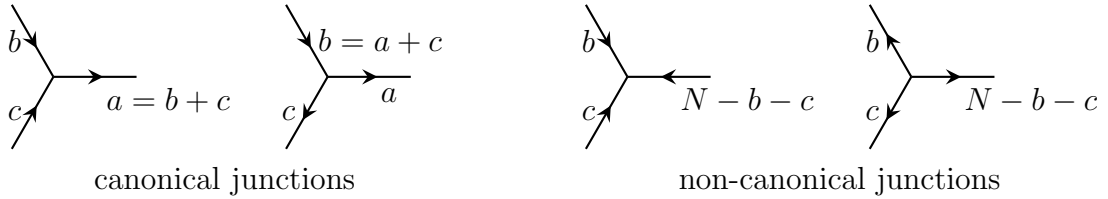


Figure 3: Canonical and non-canonical junctions

Furthermore, $\wedge^2 \square$ can be naturally embedded within $\square \otimes \square$ by the rule

$$\iota_{2 \rightarrow 1,1} : e_i \wedge e_j \mapsto -\mathfrak{q} e_i \otimes e_j + e_j \otimes e_i, \quad (i < j). \quad (3.10)$$

More generally, we associate to any canonical junction that combines labels a, b to $a + b$ the projection

$$\pi_{a,b \rightarrow a+b} : e_{i_1} \wedge \cdots \wedge e_{i_a} \otimes e_{j_1} \wedge \cdots \wedge e_{j_b} \mapsto e_{i_1} \wedge \cdots \wedge e_{i_a} \wedge e_{j_1} \wedge \cdots \wedge e_{j_b} \quad (3.11)$$

and to any canonical junction that splits the label $a + b$ to two labels a, b the map $\iota_{a+b \rightarrow a,b}$ where

$$\begin{aligned} \iota_{a+b \rightarrow a,b} : e_{k_1} \wedge \cdots \wedge e_{k_{a+b}} \\ \mapsto (-\mathfrak{q})^{ab} \sum_{i_1 < \cdots < i_a, j_1 < \cdots < j_b} (-\mathfrak{q}^{-1})^{n(i,j;k)} e_{i_1} \wedge \cdots \wedge e_{i_a} \otimes e_{j_1} \wedge \cdots \wedge e_{j_b} \end{aligned} \quad (3.12)$$

where we assume $k_1 < \cdots < k_{a+b}$, the sum is over the disjoint split of indices

$$\{k_1, \dots, k_{a+b}\} = \{i_1, \dots, i_a\} \sqcup \{j_1, \dots, j_b\}, \quad (3.13)$$

and $n(i,j;k)$ is the minimal number of adjacent transpositions to bring the sequence $i_1, \dots, i_a, j_1, \dots, j_b$ to k_1, \dots, k_{a+b} . These maps are described in more detail mathematically in [33].

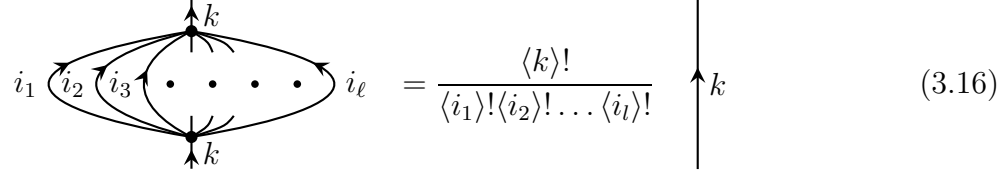
Then these maps $\pi_{a,b \rightarrow a+b}$ and $\iota_{a+b \rightarrow a,b}$ naturally combine according to the following diagrams together with the ones with reversed arrows:

or equivalently

Here $x = a + b = d - c$, $y = b + c = d - a$ and $d = a + b + c$.

3.3.2 Removal of digons

Now, we can check that any digons can be removed as



$$\text{Diagram: A network with a central digon. The top vertex is labeled } k. \text{ The edges are labeled } i_1, i_2, i_3, \dots, i_\ell. \text{ The digon has two edges labeled } k. \text{ The formula to the right is } \frac{\langle k \rangle!}{\langle i_1 \rangle! \langle i_2 \rangle! \dots \langle i_\ell \rangle!} \quad (3.16)$$

where $\sum_{a=1}^{\ell} i_a = k$.

Note that in the classical limit $\mathfrak{q} \rightarrow 1$ the prefactor becomes

$$(-1)^{\sum_{a < b} i_a i_b} \frac{k!}{i_1! i_2! \dots i_\ell!} \quad (3.17)$$

due to the fact that the classical limit of $\iota_{a+b \rightarrow a,b}$ is $(-1)^{ab}$ times the standard map that follows from the classical epsilon symbol.

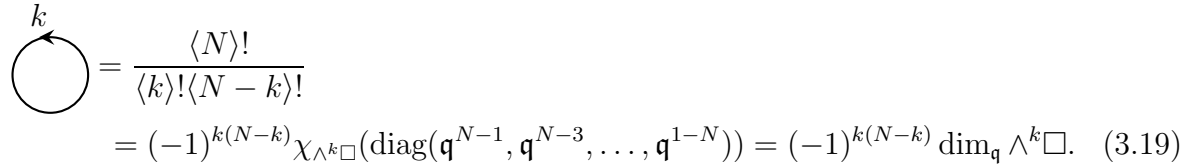
This somewhat unusual sign is however necessary to match with the known skein relations in the Liouville/Toda theory, and it also simplifies the signs appearing in the general crossing resolutions (3.36). In the q -deformed Yang-Mills theory it would be more conventional to drop this sign and the canonical junctions would be defined to be $\pi_{a,b \rightarrow a+b}$ and $(-1)^{ab} \iota_{a+b \rightarrow a,b}$. We will stick to the Liouville/Toda convention in this paper, except in Sec. 5.

When the sum of i_l is N , we can use the rule to evaluate a network with two trivalent junctions, since edges labeled by N can be removed. For example, when $i + j + k = N$, we have



$$\text{Diagram: A network with two trivalent junctions and a central circle. The top junction is labeled } i, \text{ the middle junction is labeled } j, \text{ and the bottom junction is labeled } k. \text{ The formula to the right is } \frac{\langle N \rangle!}{\langle i \rangle! \langle j \rangle! \langle k \rangle!}. \quad (3.18)$$

More simply, we can evaluate a closed loop with label k by considering it as a digon with edges labeled by k and $N - k$:



$$\text{Diagram: A closed loop with label } k. \text{ The formula to the right is } \frac{\langle N \rangle!}{\langle k \rangle! \langle N - k \rangle!} = (-1)^{k(N-k)} \chi_{\wedge^k \square}(\text{diag}(\mathfrak{q}^{N-1}, \mathfrak{q}^{N-3}, \dots, \mathfrak{q}^{1-N})) = (-1)^{k(N-k)} \dim_{\mathfrak{q}} \wedge^k \square. \quad (3.19)$$

Again, this shows that our convention is different by a factor of $(-1)^{k(N-k)}$ from the convention in the q -deformed Yang-Mills. We also see at this point that, to compare with the skein relation of the Toda theory or the q -deformed Yang-Mills theory, we need to use the relation

$$\mathfrak{q} = e^{\pi i b^2} = q_{\text{SCI}}^{1/2}. \quad (3.20)$$

3.4 Crossing resolutions

3.4.1 The \mathcal{R} matrix

Let us first discuss the best-known case: the \mathcal{R} -matrix for $\square \otimes \square$ of $SU(N)$, which is given by

$$\mathcal{R} = A(Q + \mathfrak{q}^{-1} I_{\square \otimes \square}). \quad (3.21)$$

Here, I_V is the identity operator on a vector space V , Q is an operator

$$Q = \sum_{i \neq j} e_{ij} \otimes e_{ji} - \mathfrak{q} \sum_{i < j} e_{ii} \otimes e_{jj} - \mathfrak{q}^{-1} \sum_{i > j} e_{ii} \otimes e_{jj} \quad (3.22)$$

where e_{ij} is a matrix whose only non-zero entry is 1 at the i -th row and j -th column and A is the overall normalization which we will be fixed later.

The action of Q on the base $e_a \otimes e_b$ of $\square \otimes \square$ is

$$Q(e_a \otimes e_b) = \begin{cases} e_b \otimes e_a - \mathfrak{q} e_a \otimes e_b, & (a < b) \\ 0, & (a = b) \\ e_b \otimes e_a - \mathfrak{q}^{-1} e_a \otimes e_b, & (a > b) \end{cases} \quad (3.23)$$

The resulting entries are the basis vectors of the second rank antisymmetric representation of $SU_{\mathfrak{q}}(N)$. Indeed, the operator Q is the composition of the projection $\pi_{1,1 \rightarrow 2} : \square \otimes \square \rightarrow \wedge^2 \square$ and the natural embedding $\iota_{2 \rightarrow 1,1} : \wedge^2 \square \rightarrow \square \otimes \square$:

$$Q = \iota_{2 \rightarrow 1,1} \pi_{1,1 \rightarrow 2}. \quad (3.24)$$

Note also that Q satisfies

$$Q^2 = -(\mathfrak{q} + \mathfrak{q}^{-1})Q = \langle 2 \rangle Q. \quad (3.25)$$

This is a special case of the digon elimination.

We can now represent the R-matrix \mathcal{R} diagrammatically as

$$\begin{array}{c} \diagup \quad \diagdown \\ \square \quad \square \end{array} = A \left(\begin{array}{c} \square \quad \square \\ \diagup \quad \diagdown \\ \square \quad \square \\ \diagup \quad \diagdown \\ \wedge^2 \square \\ \diagup \quad \diagdown \\ \square \quad \square \end{array} + \mathfrak{q}^{-1} \begin{array}{c} \square \\ \square \\ \square \\ \square \\ \square \\ \square \end{array} \begin{array}{c} \square \\ \square \\ \square \\ \square \\ \square \\ \square \end{array} \right). \quad (3.26)$$

The inverse of the R-matrix \mathcal{R} is

$$\mathcal{R}^{-1} = A^{-1}(Q + \mathfrak{q} I_{\square \otimes \square}) \quad (3.27)$$

that we represent as

$$\begin{array}{c} \diagup \quad \diagdown \\ \square \quad \square \end{array} = A^{-1} \left(\begin{array}{c} \square \quad \square \\ \diagup \quad \diagdown \\ \square \quad \square \\ \diagup \quad \diagdown \\ \wedge^2 \square \\ \diagup \quad \diagdown \\ \square \quad \square \end{array} + \mathfrak{q} \begin{array}{c} \square \\ \square \\ \square \\ \square \\ \square \\ \square \end{array} \begin{array}{c} \square \\ \square \\ \square \\ \square \\ \square \\ \square \end{array} \right) \quad (3.28)$$

Below, we call the crossing (3.26) as positive and the crossing (3.28) as negative.

The A_1 -case: In this case, $\wedge^2 \square$ is the trivial one-dimensional representation and there is the pseudo-reality condition $\overline{\square} \simeq \square$ which we can diagrammatically write as

$$\longrightarrow \square = \square \longleftarrow =: \text{---}. \quad (3.29)$$

Then the general equation (3.26) reduces to

$$\begin{array}{c} \diagup \diagdown \\ \diagdown \diagup \end{array} = q^{-1/2} \quad \left(\begin{array}{c} + q^{1/2} \\ \diagup \quad \diagdown \\ \diagdown \quad \diagup \end{array} \right). \quad (3.30)$$

where we have set $A = q^{1/2}$. We then have

$$q^{-1/2} \begin{array}{c} \diagup \diagdown \\ \diagdown \diagup \end{array} - q^{1/2} \begin{array}{c} \diagup \diagdown \\ \diagdown \diagup \end{array} = (q^{-1} - q) \quad \left(\begin{array}{c} \diagup \quad \diagdown \\ \diagdown \quad \diagup \end{array} \right) \quad (3.31)$$

These reproduce the standard skein relations of the Liouville theory found in [10,11] under the identification $q = e^{i\pi b^2}$.

The relation $Q^2 = \langle 2 \rangle Q$ shows

$$\text{---} = \langle 2 \rangle = -\chi_{\square}(\text{diag}(q, q^{-1})). \quad (3.32)$$

From this we see that $q = q_{\text{SCI}}^{1/2}$ where q_{SCI} is the parameter used commonly in the literature on the superconformal index. The minus sign here is a convention common in the Liouville/Toda literature, i.e. the definition of a loop in the representation \square differs by an overall minus sign between the Liouville theory and the q -deformed Yang-Mills.

The A_2 -case: Here we have $\overline{\square} = \wedge^2 \square$, and therefore we have

$$\longrightarrow \square = \wedge^2 \square \longleftarrow. \quad (3.33)$$

As we now only have one type of the label \square , we can drop it altogether. The general R-matrix (3.26) then becomes

$$\begin{array}{c} \diagup \quad \diagdown \\ \diagdown \quad \diagup \end{array} = q^{1/3} \begin{array}{c} \diagup \quad \diagdown \\ \diagdown \quad \diagup \end{array} + q^{-2/3} \begin{array}{c} \diagup \quad \diagdown \\ \diagdown \quad \diagup \end{array} \quad (3.34)$$

where we have set $A = q^{1/3}$. This reproduces the fundamental skein relations of the $\text{SU}(3)$ Toda theory found in [15], again under the identification $q = e^{i\pi b^2}$.

General case: The analysis so far suggests that we should take

$$A = \mathfrak{q}^{\frac{1}{N}} \quad (3.35)$$

in general. As we will see soon, this is consistent with the general crossing resolutions (3.36).

3.4.2 General crossing resolutions

Now let us move on to the crossing resolutions in the general case. The expression was found in [17] up to an overall factor, which we quote here:

$$\begin{array}{c} \text{Diagram of two intersecting lines with arrows labeled } a \text{ and } b \\ \diagup \quad \diagdown \\ \text{Diagram of a square with edges labeled } a-i, b-i, a+b-i, i \end{array} = \mathfrak{q}^{\frac{ab}{N}} \sum_{i=0}^s \mathfrak{q}^{-i} \quad (3.36)$$

where $s = \min(a, b, N - a, N - b)$ and $a, b = 0, 1, 2, \dots, N - 1$. With this choice of the overall factor, this equality is invariant with a reversal of an arrow and the rotation of the diagrams by 90° . Note also that when $a = b = 1$, this equality reduces to (3.26) we already discussed.

Let us introduce the names to the fundamental objects on the right hand side of (3.36):

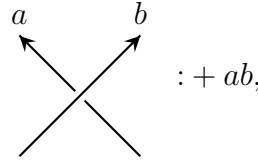
$$Q_{(i)}^{ab} := \begin{array}{c} \text{Diagram of a square with edges labeled } a-i, b-i, a+b-i, i \\ \diagup \quad \diagdown \\ \text{Diagram of a square with edges labeled } a+b-i, a-i, b, a \end{array} = \begin{array}{c} \text{Diagram of a square with edges labeled } a+b-i, a-i, b, a \\ \diagup \quad \diagdown \\ \text{Diagram of a square with edges labeled } a+b-i, a-i, b, a \end{array} \quad (3.37)$$

Note that the number of possible choices of i matches with the number of irreducible summands of the decomposition of the tensor product $\wedge^a \square \otimes \wedge^b \square$. We expect that all these $Q_{(i)}^{ab}$ cannot be further decomposed as parts of networks.

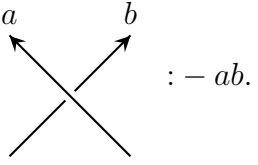
3.4.3 The intersection number and the powers of \mathfrak{q}

Let us briefly discuss the significance of the prefactor $\mathfrak{q}^{\frac{ab}{N}}$ in (3.36). In general, two loop operators in a class S theory of type $SU(N)$ can be mutually nonlocal, and the nonlocality can be measured in terms of the Dirac pairing that takes values in \mathbb{Z}_N [34]. In terms of the 2d networks realizing the 4d loop operators, the Dirac pairing is given by their intersection

number. We can define it by assigning a local intersection number to a crossing as follows:



$: + ab,$



$: - ab.$

(3.38)

This is consistent with the reversal of arrows, since it sends the label a to $N - a$.

The intersection number $I(\Gamma_1, \Gamma_2)$ of two networks Γ_1 and Γ_2 is then defined by summing the contributions from all the crossings:

$$\sum_{c : \text{crossing}} \text{sign}(c) a_c^{(1)} a_c^{(2)} \in \mathbb{Z}_N \quad (3.39)$$

where $\text{sign}(c)$ is the sign of the crossing c and $a_c^{(i)}$ is the charge of Γ_i at c .

In the Liouville/Toda setup, we expect the expectation value of any network without crossings is a single-valued function of $\mathfrak{q} = e^{\pi i b^2}$ invariant under $\mathfrak{q} \rightarrow e^{2\pi i} \mathfrak{q}$. Similarly, in the superconformal index, the expectation value of a loop operator on the 4d side is a single valued function of $\mathfrak{q} = q_{\text{SCI}}^{1/2}$, since the index is a trace $\text{Tr}(-1)^F q^{\Delta - I_3}$ and the scaling dimensions Δ of a class S theory are integral or half-integral.

Non-invariance of the expectation value under $\mathfrak{q} \rightarrow e^{2\pi i} \mathfrak{q}$ then captures the mutual non-locality, and we can think of the prefactor $\mathfrak{q}^{\frac{ab}{N}}$ in (3.36) as encoding the difference in the local intersection number between the left hand side and the right hand side, to keep track of this non-locality. The difference in the powers of \mathfrak{q} among different summands in the resolutions of the crossings should be integral, and the relation (3.36) indeed satisfies this requirement.

3.4.4 $SL(2, \mathbb{Z})$ action on the torus

We can define the operation I which we call the *inversion* by reversing all the arrows simultaneously. This is an involution that we can identify with the charge conjugation on the 4d side.

When the network is on a torus, we can also consider the action of $SL(2, \mathbb{Z})$ on the networks. Two basic actions are the T -action and the S -action. T corresponds to sending $\alpha \mapsto \alpha$, $\beta \mapsto \beta + \alpha$ and S corresponds to $\alpha \mapsto \beta$, $\beta \mapsto -\alpha$, where α, β are two bases of the 1-cycles on the torus.

The operation $C = S^2$ generates the center of $SL(2, \mathbb{Z})$ and is the charge conjugation action in the 4d $\mathcal{N}=4$ SYM theory. Then we need to have two operations, C and I , to be consistent on the torus. The relation (3.37) relating two forms of the networks representing the same object $Q_{(i)}^{ab}$ is exactly the one required to have $C = I$, when these networks are put on the torus and open edges are connected to the opposite ones.

3.5 Reidemeister moves

In knot theory, a projective representation in two dimension of knots and links in a three dimensional space is not unique, and any different representations can be mapped to each other by a combination of three so-called *Reidemeister moves*, see e.g. [35]. The move I straightens a twist in an edge, the move II slides one edge over another edge to two parallel edges, and the move III changes the order of three crossings. In the presence of junctions, we need to add another move, where we move an edge over a junction. We call this as the move IV.

Since we expect that the charge of a loop in the 4d theory is determined by the isotropy class of networks, we would like to require that a network is invariant under these moves. This is indeed possible for the moves II, III and IV, but the move I results in a q -dependent factor. In the context of 3d Chern-Simons theory, this can be understood from the change in the framing of the link [36]. Let us describe these moves explicitly below.

R-Move II: This relation says that the the negative crossing is given by the inverse \mathcal{R}^{-1} of the R-matrix \mathcal{R} corresponding to the positive crossing.

$$\begin{array}{ccc}
 \text{Diagram: two strands } V_1 \text{ and } V_2 \text{ crossing} & = & \text{Diagram: two strands } V_1 \text{ and } V_2 \text{ parallel} \\
 \text{Diagram: two strands } V_1 \text{ and } V_2 \text{ crossing} & = & \text{Diagram: two strands } V_1 \text{ and } V_2 \text{ parallel}
 \end{array} \quad (3.40)$$

R-Move III This is the Yang-Baxter equation which the R-matrix \mathcal{R} should satisfy.

$$\begin{array}{ccc}
 \text{Diagram: three strands } V_1, V_2, V_3 \text{ with a crossing} & = & \text{Diagram: three strands } V_1, V_2, V_3 \text{ with a crossing}
 \end{array} \quad (3.41)$$

R-Move IV This is the additional move for the networks with junctions.

$$\begin{array}{ccc}
 \text{Diagram: three strands } V_1, V_2, V_3 \text{ with a junction } W & = & \text{Diagram: three strands } V_1, V_2, V_3 \text{ with a junction } W \\
 \text{Diagram: three strands } V_1, V_2, V_3 \text{ with a junction } W & = & \text{Diagram: three strands } V_1, V_2, V_3 \text{ with a junction } W
 \end{array} \quad (3.42)$$

R-Move I Finally, this move involves a nontrivial factor.

$$\begin{array}{c} \text{Diagram: a vertical line with an upward arrow and a circle at the top.} \\ V \end{array} = C_V(\mathbf{q}) \begin{array}{c} \text{Diagram: a vertical line with an upward arrow.} \\ V \end{array}, \quad \begin{array}{c} \text{Diagram: a vertical line with an upward arrow and a circle at the top.} \\ V \end{array} = C_V(\mathbf{q}^{-1}) \begin{array}{c} \text{Diagram: a vertical line with an upward arrow.} \\ V \end{array}. \quad (3.43)$$

When the representation V is $\wedge^k \square$, the coefficient $C_k(\mathbf{q})$ can be calculated using the general crossing resolution (3.36) and the relation (3.16) removing digons. The i -th network on the right hand side of (3.36) gives a coefficient $\frac{(N-k+i)!}{\langle i \rangle! \langle k-i \rangle! \langle N+i-2k \rangle!}$ thanks to (3.16). We then find

$$C_k(\mathbf{q}) = (-1)^{k(N+1)} \mathbf{q}^{-(1+\frac{1}{N})k(N-k)}. \quad (3.44)$$

A direct understanding of this coefficient in 4d or 6d would be an interesting problem.

3.6 More simplifying relations

Let us list various other skein relations that can be used to simplify networks. All relations except (3.48) are known in [32] [31] and references therein.

3.6.1 Triangle contraction relations

We have rules to remove triangles. In order to express the rules, we first map all the junctions so that they are canonical. Then, there are four possibilities up to the mirror images:

$$\begin{array}{c} \text{Diagram: a triangle with vertices } b, c \text{ and a central vertex } a. \text{ Arrows } i \text{ and } j \text{ point to } a. \\ b \quad a \quad c \\ i \quad j \end{array} = \frac{\langle a \rangle!}{\langle i \rangle! \langle j \rangle!} \begin{array}{c} \text{Diagram: a triangle with vertices } b, c \text{ and a central vertex } a. \text{ Arrows } a \text{ point to } b, c. \\ b \quad a \quad c \\ a \end{array}, \quad \begin{array}{c} \text{Diagram: a triangle with vertices } b, c \text{ and a central vertex } a. \text{ Arrows } i \text{ and } j \text{ point to } a. \\ b \quad a \quad c \\ i \quad j \end{array} = \frac{\langle N-a \rangle!}{\langle N-i \rangle! \langle j \rangle!} \begin{array}{c} \text{Diagram: a triangle with vertices } b, c \text{ and a central vertex } a. \text{ Arrows } b, c \text{ point to } a. \\ b \quad a \quad c \\ b, c \end{array}, \quad (3.45)$$

$$\begin{array}{c} \text{Diagram: a triangle with vertices } b, c \text{ and a central vertex } a. \text{ Arrows } i \text{ and } j \text{ point to } a. \\ b \quad a \quad c \\ i \quad j \end{array} = \frac{\langle a \rangle!}{\langle i \rangle! \langle j \rangle!} \begin{array}{c} \text{Diagram: a triangle with vertices } b, c \text{ and a central vertex } a. \text{ Arrows } a \text{ point to } b, c. \\ b \quad a \quad c \\ a \end{array}, \quad \begin{array}{c} \text{Diagram: a triangle with vertices } b, c \text{ and a central vertex } a. \text{ Arrows } i \text{ and } j \text{ point to } a. \\ b \quad a \quad c \\ i \quad j \end{array} = \frac{\langle N-a \rangle!}{\langle i \rangle! \langle N-j \rangle!} \begin{array}{c} \text{Diagram: a triangle with vertices } b, c \text{ and a central vertex } a. \text{ Arrows } b, c \text{ point to } a. \\ b \quad a \quad c \\ b, c \end{array}. \quad (3.46)$$

Note that whether three vertices are totally ordered by arrows or not changes the look of the factors.

3.6.2 Rectangle decaying relations

The rectangles $Q_{ab}^{(i)}$ that we had in (3.37) can not be further simplified, but there are many other rectangles that are equivalent to sums of simpler ones. Let us show one class:

$$\begin{array}{ccc}
 \begin{array}{c} \text{Diagram of a rectangle with corners labeled } k, \ell, j, \ell-j, k+j, k, \ell, \ell-j, j. \end{array} & = & \sum_{s=\max(0, j-\ell+k)}^{\min(j, k)} \frac{(\ell-k)!}{(\ell-k+s-j)!(j-s)!} \begin{array}{c} \text{Diagram of a rectangle with corners labeled } k-s, \ell, s, \ell+s, k, k-s, s, \ell. \end{array} \quad (3.47)
 \end{array}$$

This is valid for $k \leq \ell$ and $0 \leq j \leq \min(k, N - \ell)$ or $k \leq j \leq \ell \leq N - k$.

These relations assure that any network constructed from only rectangles around a tube can always be decomposed into a sum of closed loops around the tube. For example, using (3.47) recursively, we can see

$$\begin{array}{ccc}
 \begin{array}{c} \text{Diagram of a rectangle with corners labeled } k, k, k, k. \end{array} & = & \mathfrak{q}^{-k} \sum_{i=-k}^k (-1)^i \mathfrak{q}^{i^2+i} \begin{array}{c} \text{Diagram of two vertical lines with corners labeled } k+i, k-i, k+i, k-i. \end{array} \quad (3.48)
 \end{array}$$

where the two horizontal thin parallel lines signify that they are to be identified so that the network is on a tube.

There are various other relations. Here we just note one example:

$$\begin{array}{ccc}
 \begin{array}{c} \text{Diagram of a rectangle with corners labeled } 3, k, k-2, 2, 1, k-1, k, 3. \end{array} & = & \langle 3 \rangle \begin{array}{c} \text{Diagram of a rectangle with corners labeled } 3, k-2, k+1, 2, 1, k, 3. \end{array} + \langle 2 \rangle \begin{array}{c} \text{Diagram of a rectangle with corners labeled } 3, k-1, k+2, 1, 2, k, 3. \end{array} \quad (3.49)
 \end{array}$$

3.7 Examples: A_2 and A_3

The skein relations of the A_1 case and the A_2 case have already been described in the literature.

3.7.1 A_2

Let us record the A_2 case as a summary. We have two types of junctions :

$$\begin{array}{ccc}
 \begin{array}{c} \text{Diagram of a junction with two inputs } 1, 2, \text{ one output } 1, \text{ and one output } 2. \end{array} & = & \begin{array}{c} \text{Diagram of a junction with two inputs } 1, 2, \text{ one output } 1, \text{ and one output } 2. \end{array} \\
 \begin{array}{c} \text{Diagram of a junction with two inputs } 1, 2, \text{ one output } 1, \text{ and one output } 2. \end{array} & = & \begin{array}{c} \text{Diagram of a junction with two inputs } 1, 2, \text{ one output } 1, \text{ and one output } 2. \end{array} \quad (3.50)
 \end{array}$$

The basic skein relation was (3.34), which we copy here [14–16]:

$$\begin{array}{c} \diagup \quad \diagdown \\ \diagdown \quad \diagup \end{array} = q^{1/3} \begin{array}{c} \diagup \quad \diagdown \\ \diagdown \quad \diagup \\ \diagup \quad \diagdown \\ \diagdown \quad \diagup \end{array} + q^{-2/3} \begin{array}{c} \uparrow \\ \uparrow \\ \uparrow \end{array} . \quad (3.51)$$

The following two relations are useful to simplify the networks:

$$\begin{array}{c} \leftarrow \circlearrowleft \end{array} = \langle 2 \rangle \quad \begin{array}{c} \leftarrow \end{array} , \quad \begin{array}{c} \diagup \quad \diagdown \\ \diagdown \quad \diagup \\ \diagup \quad \diagdown \\ \diagdown \quad \diagup \end{array} = \begin{array}{c} \uparrow \\ \uparrow \\ \uparrow \end{array} + \begin{array}{c} \uparrow \\ \leftarrow \\ \leftarrow \end{array} . \quad (3.52)$$

3.7.2 A_3

Let us now discuss the next nontrivial case of A_3 . Note that the label 3 can be traded with 1 by reversing the arrow, and since 2 is a real representation we do not have to exhibit the direction for edges labeled by 2. In this case, there are also two types of junctions as we see below.

There are three types of crossing resolutions :

$$\begin{array}{c} 1 \quad 1 \\ \diagup \quad \diagdown \\ \diagdown \quad \diagup \end{array} = q^{1/4} \begin{array}{c} 1 \quad 1 \\ \diagup \quad \diagdown \\ \diagdown \quad \diagup \\ 2 \\ \diagup \quad \diagdown \\ \diagdown \quad \diagup \\ 1 \quad 1 \end{array} + q^{-3/4} \begin{array}{c} 1 \\ \uparrow \\ 1 \end{array} , \quad (3.53)$$

$$\begin{array}{c} 1 \quad 2 \\ \diagup \quad \diagdown \\ \diagdown \quad \diagup \end{array} = q^{1/2} \begin{array}{c} 1 \quad 2 \\ \diagup \quad \diagdown \\ \diagdown \quad \diagup \\ 3 \\ \diagup \quad \diagdown \\ \diagdown \quad \diagup \\ 2 \quad 1 \end{array} + q^{-1/2} \begin{array}{c} 1 \quad 2 \\ \diagup \quad \diagdown \\ \diagdown \quad \diagup \\ 2 \\ \diagup \quad \diagdown \\ \diagdown \quad \diagup \\ 1 \quad 1 \end{array} , \quad (3.54)$$

$$\begin{array}{c} 2 \quad 2 \\ \diagup \quad \diagdown \\ \diagdown \quad \diagup \end{array} = q \begin{array}{c} 2 \quad 2 \\ \diagup \quad \diagdown \\ \diagdown \quad \diagup \\ 2 \\ \diagup \quad \diagdown \\ \diagdown \quad \diagup \\ 2 \quad 2 \end{array} + \begin{array}{c} 2 \quad 2 \\ \diagup \quad \diagdown \\ \diagdown \quad \diagup \\ 1 \\ \diagup \quad \diagdown \\ \diagdown \quad \diagup \\ 1 \quad 3 \\ \diagup \quad \diagdown \\ \diagdown \quad \diagup \\ 1 \quad 1 \\ \diagup \quad \diagdown \\ \diagdown \quad \diagup \\ 2 \quad 2 \end{array} + q^{-1} \begin{array}{c} 2 \\ \uparrow \\ 2 \end{array} . \quad (3.55)$$

There are three decaying relations for one rectangle:

$$\begin{array}{c} 2 \quad 1 \\ \diagup \quad \diagdown \\ \diagdown \quad \diagup \\ 1 \quad 2 \\ \diagup \quad \diagdown \\ \diagdown \quad \diagup \\ 1 \quad 1 \end{array} = \begin{array}{c} 2 \\ \uparrow \\ 1 \end{array} + \begin{array}{c} 2 \quad 1 \\ \diagup \quad \diagdown \\ \diagdown \quad \diagup \\ 1 \\ \diagup \quad \diagdown \\ \diagdown \quad \diagup \\ 1 \quad 1 \end{array} , \quad (3.56)$$

$$\begin{array}{c}
\text{Diagram: } \begin{array}{c} 1 & & 1 \\ & \swarrow & \searrow \\ & 1 & \\ & \uparrow & \downarrow \\ 1 & & 1 \end{array} \quad = \langle 2 \rangle \quad \downarrow \quad 1 \quad + \quad \begin{array}{c} 1 \\ \longrightarrow \\ 1 \end{array} \quad , \\
\text{Diagram: } \begin{array}{c} 1 & & 1 \\ & \swarrow & \searrow \\ & 1 & \\ & \uparrow & \downarrow \\ 1 & & 1 \end{array} \quad = \langle 2 \rangle \quad \begin{array}{c} 1 \\ \nearrow \\ 1 \end{array} \quad \begin{array}{c} 2 \\ \nearrow \\ 1 \end{array} \quad \begin{array}{c} 1 \\ \nearrow \\ 1 \end{array} \quad .
\end{array}$$

$$\begin{array}{c}
\text{Diagram: } \begin{array}{c} 1 & & 1 \\ & \swarrow & \searrow \\ & 1 & \\ & \uparrow & \downarrow \\ 1 & & 1 \end{array} \quad = \langle 2 \rangle \quad \downarrow \quad 1 \quad + \quad \begin{array}{c} 1 \\ \longrightarrow \\ 1 \end{array} \quad , \\
\text{Diagram: } \begin{array}{c} 1 & & 1 \\ & \swarrow & \searrow \\ & 1 & \\ & \uparrow & \downarrow \\ 1 & & 1 \end{array} \quad = \langle 2 \rangle \quad \begin{array}{c} 1 \\ \nearrow \\ 1 \end{array} \quad \begin{array}{c} 2 \\ \nearrow \\ 1 \end{array} \quad \begin{array}{c} 1 \\ \nearrow \\ 1 \end{array} \quad .
\end{array}$$

4 Networks for $\mathcal{N}=4$ Yang-Mills

As the fundamental aspects of defect networks in the two dimensional theories have been discussed, we can move on to the discussion of the correspondence between networks on the 2d side and loops on the 4d side. In this section, we restrict ourselves to the most familiar $\mathcal{N}=4$ case. On the gauge theory side, the charges of the loop operators were classified in [21]. It is not easy to construct the corresponding networks for the general A_k case, but we will see that the skein relations allow us to describe and classify the networks for A_2 concretely.

Before proceeding, let us quickly recall the possible charges of the loop operators of $\mathcal{N}=4$ $SU(N)$ Yang-Mills, following [21]. We denote the weight lattice by Λ . We use the notations ω_i for the fundamental weights and h_i for the weight vectors in the defining N -dimensional representation. They are explicitly given by

$$\omega_i = (1 - \frac{i}{N}, \dots, 1 - \frac{i}{N}, -\frac{i}{N}, \dots, -\frac{i}{N}), \quad (4.1)$$

$$h_i = (-\frac{1}{N}, \dots, -\frac{1}{N}, 1 - \frac{1}{N}, -\frac{1}{N}, \dots, -\frac{1}{N}). \quad (4.2)$$

Note that $\omega_1 = h_1$ and $\omega_{N-1} = -h_N$.

Let us consider a Wilson loop labeled by an irreducible representation R . We can also use its highest weight λ as the label, and possible highest weights are in one-to-one correspondence with Λ/\mathcal{W} where \mathcal{W} is the Weyl group. Similarly, a 't Hooft loop can be characterized by a charge vector in Λ , considered up to the action of the Weyl group.

For a dyonic loop operator, we need to specify a pair of electric and magnetic charges $(\mu, \lambda) \in \Lambda \times \Lambda$ but the charges need to be identified under a simultaneous action of the Weyl group. Therefore a dyonic charge corresponds to an element in $(\Lambda \times \Lambda)/\mathcal{W}$ and represent the element as $[(\mu, \lambda)]$. We also call it $[(\mu', \lambda')] \text{ lower than } [(\mu, \lambda)]$ if μ' and λ' are lower than μ and λ respectively when mapped to Λ/\mathcal{W} .

4.1 The product of Wilson loops and 't Hooft loops

It is well known how pure Wilson loops and pure 't Hooft loops are represented as loops on the torus :

$$W_{\omega_a} \iff \begin{array}{c} \text{parallelogram} \\ \text{horizontal edge} \xrightarrow{a} \end{array}, \quad T_{\omega_b} \iff \begin{array}{c} \text{parallelogram} \\ \text{vertical edge} \xrightarrow{b} \end{array} \quad (4.3)$$

where we identify each pair of parallel opposite edges to make the parallelogram the torus. Here W_R is the Wilson loop in the representation R , and we identify an irreducible representation and its highest weight vector. We use a similar notation for the 't Hooft loop. We also fix the horizontal one cycle as α -cycle and the vertical one as β -cycle. Note that the S transformation on the torus is naturally identified with S duality transformation of $\mathcal{N}=4$ gauge theory.

We can now decompose the product $W_{\omega_a} \cdot T_{\omega_b}$ using the crossing resolution (3.36). Here we express it in a form to make the data of electromagnetic charges manifest:

$$\begin{array}{c} \text{crossing} \\ \text{horizontal edge} \xrightarrow{b} \\ \text{vertical edge} \xrightarrow{a} \end{array} = \sum_{[(\mu_b^{(i)}, \lambda_a^{(i)})] \in \mathcal{D}(\omega_b, \omega_a)} q^{-\langle \mu_b^{(i)}, \lambda_a^{(i)} \rangle} \begin{array}{c} \text{square} \\ \text{horizontal edges} \xrightarrow{b-i} \\ \text{vertical edges} \xrightarrow{i} \\ \text{diagonal edges} \xrightarrow{a-b-i} \\ \text{bottom edge} \xrightarrow{a-i} \\ \text{right edge} \xrightarrow{b} \end{array} \quad (4.4)$$

where

$$\mathcal{D}(\mu, \lambda) := (\mathcal{W}(\mu) \times \mathcal{W}(\lambda)) / \mathcal{W} \quad (4.5)$$

is the set parameterizing the possible ways to combine a magnetic charge $\mathcal{W}(\mu)$ Weyl-conjugate to μ and an electric charge $\mathcal{W}(\nu)$ Weyl-conjugate to ν .

The number of elements in the set $\mathcal{D}(\omega_b, \omega_a)$ is given by $s = \min(a, b, N - a, N - b)$ and is in a one-to-one correspondence with the label i in the summation (3.36). The label i and a representative $[(\mu_b^{(i)}, \lambda_a^{(i)})] \in \mathcal{D}(\omega_b, \omega_a)$ can be naturally related by the equation

$$i = \frac{ab}{N} + \langle \mu_b^{(i)}, \lambda_a^{(i)} \rangle. \quad (4.6)$$

Recalling the fact reviewed in Sec. 2.2 and that $\langle \mu_b^{(i)}, \lambda_a^{(i)} \rangle$ is the x -component of the classical angular momentum associated to the Poynting vector under electric charge $\lambda_a^{(i)}$ and magnetic charge $\mu_b^{(i)}$ in the Coulomb phase with the gauge group $U(1)^{N-1}$, we naturally expect the following correspondence : ⁶

$$\begin{array}{c} \text{crossing} \\ \text{horizontal edge} \xrightarrow{b} \\ \text{vertical edge} \xrightarrow{a} \\ \text{diagonal edge} \xrightarrow{i} \end{array} \iff D_{[(\mu_b^{(i)}, \lambda_a^{(i)})]} \quad (4.7)$$

⁶There are other three equivalent networks connected to each other under (3.14) or (3.15).

where we use the symbol $D_{[(\mu, \nu)]}$ to denote the dyonic loop operator with the charge $[(\mu, \nu)] \in (\Lambda \times \Lambda)/\mathcal{W}$. We also use a simple symbol $D_{(i)}^{b,a}$ for $D_{[(\mu_b^{(i)}, \lambda_a^{(i)})]}$. Below, we call these dyonic loops $D_{(i)}^{b,a}$ and the corresponding networks *elementary*.

4.2 Analysis in the Liouville/Toda theory

Let us now connect our analysis so far with a computation on the Liouville/Toda theory side, using the localization in the gauge theory [30, 37].

Hereafter we use symbols $a = (a_1, a_2, \dots, a_N)$ under the constraint $\sum_{i=1}^N a_i = 0$, $A_i(a) := \exp[2\pi i b \langle a, h_i \rangle]$ and $A(a) = \text{diag}(A_1(a), A_2(a), \dots, A_N(a))$. We also denote the $\mathcal{N}=4$ holomorphic partition function by $\mathcal{Z}(a)$.

As seen in [37] and [30], Wilson loop W_R and 't Hooft loop T_R are written in the form of matrix model :

$$\langle W_R \rangle = \int_{i\mathbb{R}^{N-1}} [da] \mathcal{Z}(a)^* \chi_R(A(a)) \mathcal{Z}(a), \quad (4.8)$$

$$\langle T_R \rangle = \int_{i\mathbb{R}^{N-1}} [da] \mathcal{Z}(a)^* \sum_{\lambda \in \Pi(R)} T_\lambda^{(R)}(a) \mathcal{Z}(a - b\lambda) \quad (4.9)$$

where χ_R is the character of R and $\Pi(R)$ is the set of weights corresponding to the irreducible representation R . $T_\lambda^{(R)}(a)$ are some functions of a related to the character χ_R via a Fourier transformation in a [12, 30] but the concrete expressions are unnecessary hereafter.

In general, any loop operator is expected to be represented as

$$\langle X \rangle = \int_{i\mathbb{R}^{N-1}} [da] \mathcal{Z}(a)^* \sum_{\nu} X_\nu(a) \mathcal{Z}(a - b\nu) \quad (4.10)$$

where ν runs over some finite set in the weight lattice Λ and $X_\nu(a)$ are some functions the detail of which we do not need either. The additions of W_R and T_R in the ordering of loops seen in Sec. 2.1 are written as follows :

$$\begin{aligned} \langle W_R X \rangle &= \int_{i\mathbb{R}^{N-1}} [da] \mathcal{Z}(a)^* W_R \sum_{\nu} X_\nu(a) \mathcal{Z}(a - b\nu) \\ &= \int_{i\mathbb{R}^{N-1}} [da] \mathcal{Z}(a)^* \sum_{\nu} X_\nu(a) \chi_R(A(a - b\nu)) \mathcal{Z}(a - b\nu), \end{aligned} \quad (4.11)$$

$$\begin{aligned} \langle T_R X \rangle &= \int_{i\mathbb{R}^{N-1}} [da] \mathcal{Z}(a)^* T_R \sum_{\nu} X_\nu(a) \mathcal{Z}(a - b\nu) \\ &= \int_{i\mathbb{R}^{N-1}} [da] \mathcal{Z}(a)^* \sum_{\mu \in \Pi(R)} \sum_{\nu} T_\mu^{(R)}(a - b\nu) X_\nu(a) \mathcal{Z}(a - b\nu - b\mu). \end{aligned} \quad (4.12)$$

In particular, let us choose R as one of the fundamental representations $\wedge^n \square$ and introduce $W^{(k)} := W_{\wedge^k \square}$ and $T^{(\ell)} := T_{\wedge^\ell \square}$. Then consider insertions both of $W^{(k)}$ and of

$T^{(\ell)}$. One way to insert is

$$\langle \cdots T^{(\ell)} W^{(k)} X \rangle = \int_{i\mathbb{R}^{N-1}} [da] \mathcal{Z}(a)^* \cdots \sum_{\mu \in \Pi(\wedge^\ell \square)} \sum_{\nu} T_\mu^{(\ell)}(a - b\nu) X_\nu(a) \chi_{\wedge^k \square}(A(a - b\nu)) \mathcal{Z}(a - b\nu - b\mu) \quad (4.13)$$

where the ellipsis represents further insertions of other loops.

Recalling $\chi_R(A(a)) = \sum_{\lambda \in \Pi(R)} \exp[2\pi i b \langle a, \lambda \rangle]$, then define the following operators labeled by $m = 1, 2, \dots, \min(k, \ell)$:

$$\langle \cdots [TW]_m^{(\ell, k)} X \rangle := \int_{i\mathbb{R}^{N-1}} [da] \mathcal{Z}(a)^* \cdots \sum_{(\lambda, \mu) \in \Pi(\wedge^\ell \square, \wedge^k \square)_m} \sum_{\nu} T_\mu^{(\ell)}(a - b\nu) X_\nu(a) \exp[2\pi i b \langle a - b\nu, \lambda \rangle] \mathcal{Z}(a - b\nu - b\mu). \quad (4.14)$$

where we decompose the set $\Pi(\wedge^\ell \square) \times \Pi(\wedge^k \square) = \mathcal{W}(\omega_\ell) \times \mathcal{W}(\omega_k)$ into several sectors defined by

$$\Pi(\wedge^\ell \square, \wedge^k \square)_m := \{(\mu, \lambda) \in \Pi(\wedge^\ell \square) \times \Pi(\wedge^k \square) \mid \langle \mu, \lambda \rangle = m - \frac{k\ell}{N}\} = \mathcal{D}(\omega_\ell, \omega_k). \quad (4.15)$$

We then have

$$\langle \cdots T^{(\ell)} W^{(k)} X \rangle = \sum_m \langle \cdots [TW]_m^{(\ell, k)} X \rangle. \quad (4.16)$$

Note that the decomposition of $T^{(\ell)} W^{(k)}$ is independent of the ellipsis \dots and X assuring that this expansion is local and represent the product as $T^{(\ell)} \cdot W^{(k)}$ or $T^{(\ell)} \times W^{(k)}$.

On the other hand, the insertion in the opposite order is

$$\langle \cdots W^{(k)} T^{(\ell)} X \rangle = \int_{i\mathbb{R}^{N-1}} [da] \mathcal{Z}(a)^* \cdots \sum_{\mu \in \Pi(\wedge^\ell \square)} \sum_{\nu} T_\mu^{(\ell)}(a - b\nu) X_\nu(a) \chi_{\wedge^k \square}(A(a - b\mu - b\nu)) \mathcal{Z}(a - b\nu - b\mu) \quad (4.17)$$

and we also have

$$\langle \cdots T^{(\ell)} W^{(k)} X \rangle = \sum_m \langle \cdots \mathfrak{q}^{2\left(\frac{k\ell}{N} - m\right)} [TW]_m^{(\ell, k)} X \rangle \quad (4.18)$$

where we use

$$\exp[2\pi i b \langle a - b\mu - b\nu, \lambda \rangle] = \mathfrak{q}^{2\left(\frac{k\ell}{N} - m\right)} \exp[2\pi i b \langle a - b\nu, \lambda \rangle]. \quad (4.19)$$

In summary, we have found the relations

$$T^{(\ell)} \times W^{(k)} = \sum_{m=0}^{\min(k,\ell)} [TW]_m^{(\ell,k)}, \quad W^{(k)} \times T^{(\ell)} = \sum_{m=0}^{\min(k,\ell)} \mathfrak{q}^{2\binom{k\ell}{N}-m} [TW]_m^{(\ell,k)}. \quad (4.20)$$

Comparing the product expansion (4.20) and the graphical expansion (4.4) we find the following identification :

$$\begin{array}{cccc} (Q^{\ell k} \text{ on } T^2) & \leftrightarrow & D_{(m)}^{\ell,k} & \leftrightarrow \\ \text{network} & & 4\text{d loop} & \text{charge} \\ & & & \text{operator} \end{array} \quad (4.21)$$

Here the pair of weights $[(\mu_\ell^{(m)}, \lambda_k^{(m)})]$ was chosen as in (4.4), and therefore we have $\langle \mu_\ell^{(m)}, \lambda_k^{(m)} \rangle = m - \frac{k\ell}{N}$.

Let us see how T transformation of the $SL(2, \mathbb{Z})$ duality action acts on these loop operators. The θ dependence originally comes from the classical part of $\mathcal{N}=4$ partition function $\mathcal{Z}(a) = \exp[-\pi i \tau \langle a, a \rangle]$ where holomorphic gauge coupling $\tau = \frac{\theta}{2\pi} + \frac{4\pi i}{g_{YM}^2}$ and the monodromy action under the change $\theta \rightarrow \theta + 2\pi$ is following :

$$\begin{aligned} \mathcal{Z}(a)^* \mathcal{Z}(a - b\lambda) &\xrightarrow{\tau \rightarrow \tau + 1} \exp[-\pi i(\langle a - b\lambda, a - b\lambda \rangle - \langle a, a \rangle)] \mathcal{Z}(a)^* \mathcal{Z}(a - b\lambda) \\ &= \mathfrak{q}^{-\langle \lambda, \lambda \rangle} e^{2\pi i b \langle \lambda, a \rangle} \mathcal{Z}(a)^* \mathcal{Z}(a - b\lambda) \end{aligned} \quad (4.22)$$

The Witten effect on the partition function can be re-expressed in the loop operators which acts on the partition functions. In particular, when λ is in $\Pi(\wedge^\ell \square) = \mathcal{W}(\omega_\ell)$, $\mathcal{Z}(a)^* \mathcal{Z}(a - b\lambda)$ is accompanied by

$$\mathfrak{q}^{-\ell + \frac{\ell^2}{N}} e^{2\pi i b \langle \lambda, a \rangle} \quad (4.23)$$

as θ shifts by 2π . Summing it up over $\Pi(\wedge^\ell \square)$,

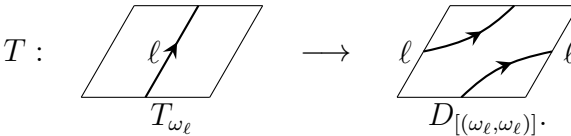
$$T^{(\ell)} \longrightarrow \mathfrak{q}^{-\ell + \frac{\ell^2}{N}} [TW]_\ell^{(\ell,\ell)} = D_{[(\omega_\ell, \omega_\ell)]} = D_{(\ell)}^{\ell,\ell} \quad (4.24)$$

under $\theta \rightarrow \theta + 2\pi$. Since $D_{[(\omega_\ell, \omega_\ell)]} = D_{(\ell)}^{\ell,\ell}$ is given by



$$(4.25)$$

This $\theta \rightarrow \theta + 2\pi$ action is graphically represented as



$$T : \quad \begin{array}{c} \text{square} \\ \text{top-left line labeled 'l'} \\ \text{bottom-right line labeled 'l'} \end{array} \quad \rightarrow \quad \begin{array}{c} \text{square} \\ \text{top-left line labeled 'l'} \\ \text{bottom-right line labeled 'l'} \end{array} \quad D_{[(\omega_\ell, \omega_\ell)]}. \quad (4.26)$$

and matches with the T transformation on the torus.

4.3 Examples of products of loops in A_2

Let us focus on the A_2 case and perform some explicit computations. The examples in the general A_k case will be given in Appendix A. We will see the geometric $SL(2, \mathbb{Z})$ action on the torus is nicely mapped to the $SL(2, \mathbb{Z})$ action on the electric and magnetic weight systems.

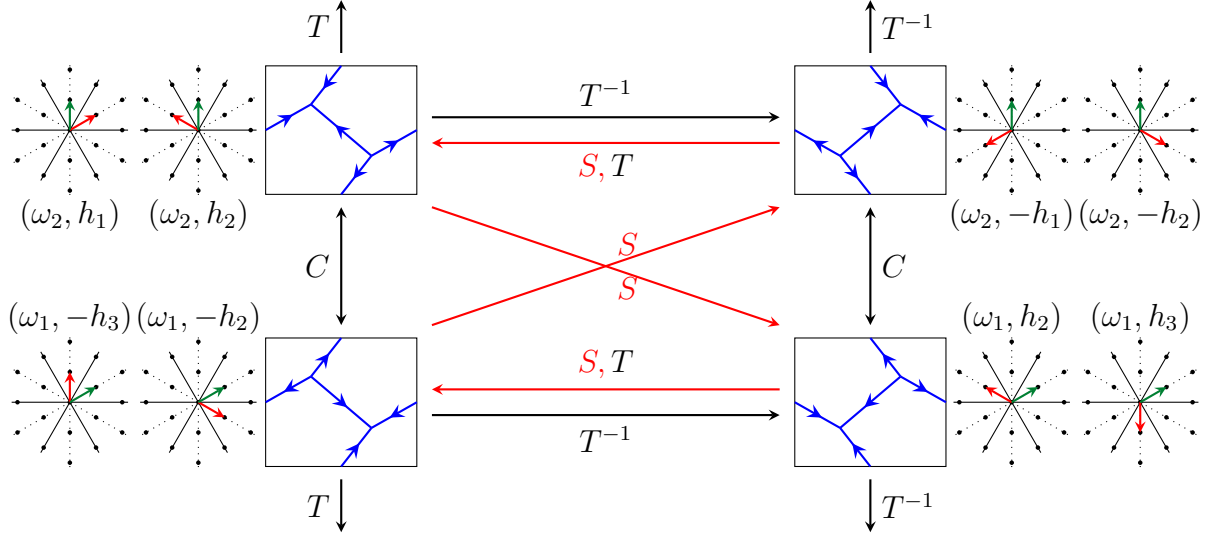


Figure 4: The $SL(2, \mathbb{Z})$ duality orbit of $D_{(0)}^{1,1}$ (below right) and their dyonic charges. Two adjacent expressions of a pair of weights are equivalent via some Weyl reflections. Red weights correspond to electric weights and green's to magnetic ones.

Example 1. The simplest case is $W_{\square} \times T_{\square}$, which corresponds to the equation (4.4) with $a = 1$ and $b = 1$:

$$W_{\square} \times T_{\square} = \mathfrak{q}^{1/3} D_{(0)}^{1,1} + \mathfrak{q}^{-2/3} D_{(1)}^{1,1} \quad (4.27)$$

where $D_{(0)}^{1,1} = D_{[(\omega_1, h_2)]} = D_{[(\omega_1, h_3)]}$ and $D_{(1)}^{1,1} = D_{[(\omega_1, \omega_1)]}$. This was originally found in [14, 15] in the context of class S theory.

The dyonic loop $D_{(1)}^{1,1}$ is obtained from the 't Hooft loop T_{\square} by an application of the T operation. In particular this loop can be mapped to a Wilson loop in some duality frame. The object $D_{(0)}^{1,1}$ cannot be mapped into a network localized on any one cycle by the torus modular transformations. In the language of charges, this means that the electric weight and the magnetic weight are not parallel. We can now work out how the $SL(2, \mathbb{Z})$ transformations act on this particular network and the pair of weights, see Fig.4.

Example 2. The next example is $W_{\square\square} \times T_{\square}$:

$$\begin{array}{c}
\text{Diagram with a square boundary, a red horizontal line, and a green vertical line with arrows.} \\
\text{Diagram with a square boundary and a red horizontal line.} \\
= \mathfrak{q}^{2/3} \left[\begin{array}{c}
\text{Diagram with a square boundary, a red horizontal line, and a green vertical line with arrows.} \\
- \quad \text{Diagram with a square boundary and a red horizontal line.} \\
+ \mathfrak{q}^{-1} \quad \text{Diagram with a square boundary, a red horizontal line, and a green vertical line with arrows.} \\
+ \mathfrak{q}^{-2} \quad \text{Diagram with a square boundary, a red horizontal line, and a green vertical line with arrows.}
\end{array} \right].
\end{array} \quad (4.28)$$

In this example, the first term on the right hand side is a network that cannot be mapped by $SL(2, \mathbb{Z})$ to any of the networks we already studied explicitly. It is natural to posit the following expansion

$$\begin{aligned}
W_{\square} \times T_{\square} = & \mathfrak{q}^{2/3} D_{[(\omega_1, 2h_2)]} + \mathfrak{q}^{-1/3} D_{[(\omega_1, h_1 + h_2)]} + \mathfrak{q}^{-4/3} D_{[(\omega_1, 2\omega_1)]} \\
& + (\text{loops with lower weights})
\end{aligned} \quad (4.29)$$

since we expect that the exponent of \mathfrak{q} multiplying $D_{[(\lambda_m, \lambda_e)]}$ equals $-\langle \lambda_m, \lambda_e \rangle$ to capture the angular momentum. Then we can identify

$$D_{[(\omega_1, 2h_2)]} \sim \text{Diagram with a square boundary, a red horizontal line, and a green vertical line with arrows.} \quad (4.30)$$

up to the lower contribution $D_{[(\omega_1, h_i + h_{j(>i)})]}$ from lower weights. Hereafter, we try to map networks and charges of the dyonic loops up to the contributions from lower weights.⁷

Example 3. The third example is $W_{\text{Adj}} \times T_{\square}$: The skein relation gives us

$$\begin{array}{c}
\text{Diagram with a square boundary, a red horizontal line, and a green vertical line with arrows.} \\
\text{Diagram with a square boundary and a red horizontal line.} \\
\text{Adj} = \mathfrak{q} \quad + \quad \text{Diagram with a square boundary, a red horizontal line, and a green vertical line with arrows.} \\
+ \quad \text{Diagram with a square boundary, a red horizontal line, and a green vertical line with arrows.} \\
+ \mathfrak{q}^{-1} \quad \text{Diagram with a square boundary, a red horizontal line, and a green vertical line with arrows.}
\end{array} \quad (4.31)$$

while from gauge theory we expect

$$\begin{aligned}
W_{\text{Adj}} \times T_{\square} = & \mathfrak{q} D_{[(\omega_1, h_2 - h_1)]} + D_{[(\omega_1, h_1 + 2h_2)]} + \mathfrak{q}^{-1} D_{[(\omega_1, 2h_1 + h_2)]} \\
& + (\text{loops with lower weights}).
\end{aligned} \quad (4.32)$$

⁷The complication comes from two sources. One is common with what we encountered in Sec. 3.2: irreducible representations are linear combinations of networks even in the Wilson loop case. Another is related to the bubbling effect of the monopole moduli space. See the related works to this subject [30, 38–40].

For a graphical representation of weights involved, see Fig. 5.

The first term and the third term can be obtained by $SL(2, \mathbb{Z})$ transformations on $D_{(0)}^{1,1}$. The second term is a new type:

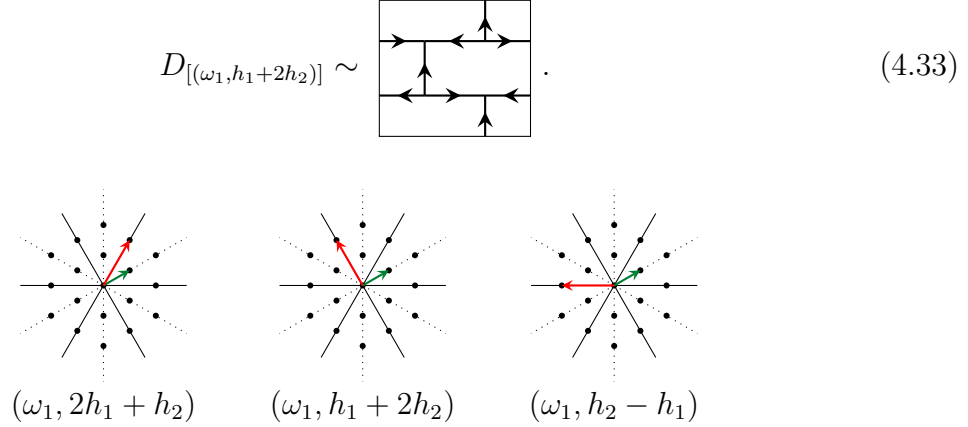


Figure 5: Representative weights in $\mathcal{D}(\omega_1, \omega_1 + \omega_2)$

Example 4. Our final example is $W_{\text{Adj}} \times T_{\text{Adj}}$. The skein relation gives

$$\begin{aligned}
 \text{Adj} & \\
 \begin{array}{c} \text{Adj} \\ \boxed{\text{Adj}} \end{array} & \text{Adj} = 4(2 + \mathfrak{q}^2 + \mathfrak{q}^{-2}) \quad \boxed{} + \\
 2 \quad \begin{array}{c} \text{Adj} \\ \boxed{} \end{array} & + 2 \quad \begin{array}{c} \text{Adj} \\ \boxed{} \end{array} + \mathfrak{q}^{-2} \quad \begin{array}{c} \text{Adj} \\ \text{Adj} \end{array} + \mathfrak{q}^2 \quad \begin{array}{c} \text{Adj} \\ \text{Adj} \end{array} \\
 + \mathfrak{q}^{-1} \left(\begin{array}{c} \text{Adj} \\ \text{Adj} \end{array} \right) & + \left(\begin{array}{c} \text{Adj} \\ \text{Adj} \end{array} \right) + \mathfrak{q} \left(\begin{array}{c} \text{Adj} \\ \text{Adj} \end{array} \right) + \left(\begin{array}{c} \text{Adj} \\ \text{Adj} \end{array} \right) \quad (4.34)
 \end{aligned}$$

while the gauge theory computation yields

$$\begin{aligned}
 W_{\text{Adj}} \times T_{\text{Adj}} &= \mathfrak{q}^{-2} D_{[(\lambda_{\text{Adj}}, \lambda_{\text{Adj}})]} + \mathfrak{q}^2 D_{[(\lambda_{\text{Adj}}, -\lambda_{\text{Adj}})]} \\
 &+ \mathfrak{q}^{-1} D_{[(\lambda_{\text{Adj}}, \lambda_{1+})]} + \mathfrak{q}^{-1} D_{[(\lambda_{\text{Adj}}, \lambda_{2+})]} + \mathfrak{q} D_{[(\lambda_{\text{Adj}}, \lambda_{2-})]} + \mathfrak{q} D_{[(\lambda_{\text{Adj}}, \lambda_{1-})]} \\
 &+ (\text{loops with the lower weights}) \quad (4.35)
 \end{aligned}$$

where $\lambda_{\text{Adj}} = \omega_1 + \omega_2$ is the highest weight of the adjoint representation and see Fig. 6 for $\lambda_{1,2\pm}$. It would be interesting to reproduce the terms with lower weights from a purely 4d gauge theoretic computations.

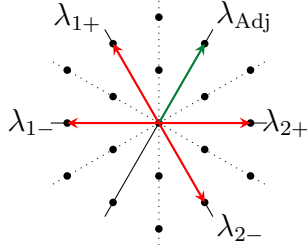


Figure 6: Representative weights in $\mathcal{D}(\omega_1 + \omega_2, \omega_1 + \omega_2)$

4.4 Classification of networks on T^2 for A_2

We have seen some basic examples of products of loops and the identification of the charge and the network. Here we establish the general mapping between the networks and the charges in the case of the A_2 theory on the torus, or equivalently the $\mathcal{N}=4$ SU(3) Yang-Mills. This is a minimal extension of the dictionary of Drukker, Morrison and Okuda [8].

Let us first classify the possible A_2 networks on the torus purely in terms of the skein relation. First, recall that all networks with crossings are resolved into those with junctions only. In particular, for the A_2 case, there are only two types of junctions, namely the one where the heads of three arrows meet and another one where the tails of three arrows meet. Therefore the networks are bipartite [14] and there appear only polygons with degree-even vertices.

We now use the skein relations we discussed so far. Recall the basic conventions we discussed in Sec. 3.7. All digons can be contracted, and all rectangles are resolved to two pairs of curves, as we discussed in (3.52).

At this point, the network might contain several disconnected components. If there are no vertices at all, the network consists of parallel loops wrapping the same one-cycle on T^2 . Assume now there is at least one vertex. Pick a connected component. It has the topology of either a disk, an annulus or a torus.

Now, let us denote the number of edges, or equivalently the number of vertices, of the i -th polygon in this connected component by $p_i (= 2, 4, 6, \dots)$. Denote the number of polygons by f . The total number of vertices, edges and faces of the network is then given by

$$V = \frac{1}{3} \sum_i p_i, \quad E = \frac{1}{2} \sum_i p_i, \quad F = f. \quad (4.36)$$

Furthermore, denote the number of boundary edges by B which vanish if the connected component has the topology of torus. From Euler's theorem we should have

$$\chi + \frac{1}{6}B = V - E + F = F - \frac{1}{6} \sum_i p_i \geq 0 \quad (4.37)$$

since the connected component is either a disk ($\chi = 1, B > 0$), an annulus ($\chi = 0, B > 0$), or a torus ($\chi = 0, B = 0$). Since we removed all digons and rectangles, $p_i \geq 6$, and

therefore we have

$$F - \frac{1}{6} \sum_i p_i \leq 0. \quad (4.38)$$

From this we see that the connected component has the topology of the torus, and every polygon is a hexagon. Therefore, the possible A_2 networks on T^2 are mapped into the bipartite hexagon tilings with three corner condition at every vertex.

It is interesting to note at this point that bipartite hexagon tilings of the torus appeared in the string theory literature in the context of brane tilings [41–43]. In this case the bipartite hexagon tilings corresponded to Abelian orbifolds of \mathbb{C}^3 .

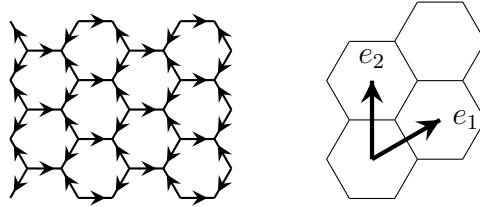


Figure 7: The infinite bipartite hexagonal tiling and its basis vectors

Now let us make the dictionary between the bipartite hexagon tilings and the dyonic charges. Instead of thinking of filling a torus by hexagons, we can take the quotient of the bipartite hexagon tiling filling the entire plane, and then we define the vectors e_1 and e_2 there, see Fig.7. To specify a bipartite hexagon tiling, we choose the α and the β cycles of the torus from $\mathbb{Z}e_1 \oplus \mathbb{Z}e_2$ so that they are linearly independent. In Fig. 8 we show the hexagonal tilings and the dyonic charges that already appeared in our analysis so far.

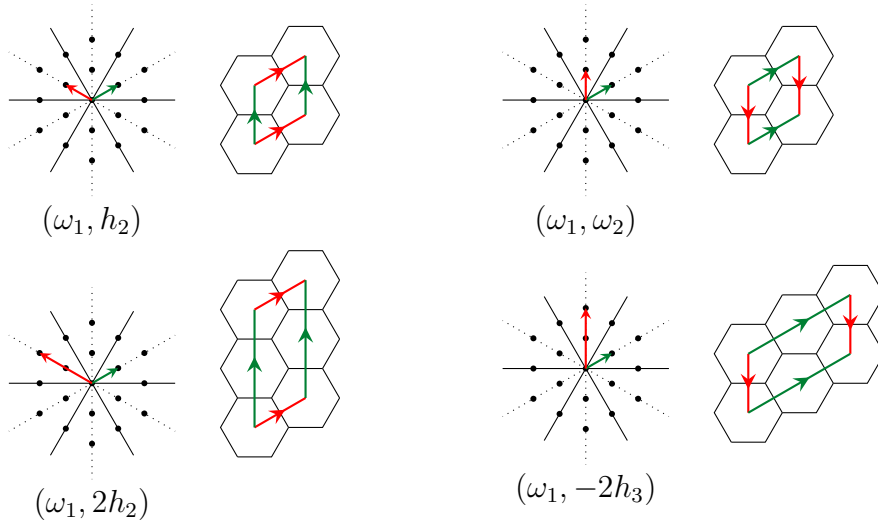


Figure 8: Some examples of the hexagonal tilings and the dyonic charges that we have already identified

From these examples, we can find the general map. We first naturally identify the A_2 weight lattice Λ and the dual lattice of the hexagonal tiling. Then, the rule is

$$(\lambda_e, \lambda_m) \mapsto (\alpha, \beta) = (\lambda_m, -\lambda_e). \quad (4.39)$$

under the condition $q_1 p_2 - q_2 p_1 > 0$ where $\lambda_e = q_1 \omega_1 + q_2 \omega_2$ and $\lambda_m = p_1 \omega_1 + p_2 \omega_2$.

It is clear that the action of the Weyl group is consistent. Because the cycles α, β define the basis of charges, the action of $SL(2, \mathbb{Z})$ on the dyonic charges (λ_e, λ_m) and that on the cycles (α, β) should be transpose of each other, and indeed the mapping (4.39) satisfies this condition. Let us end this section by exhibiting some more examples of the mapping between the dyonic charges and the hexagonal tilings, see Fig. 9.

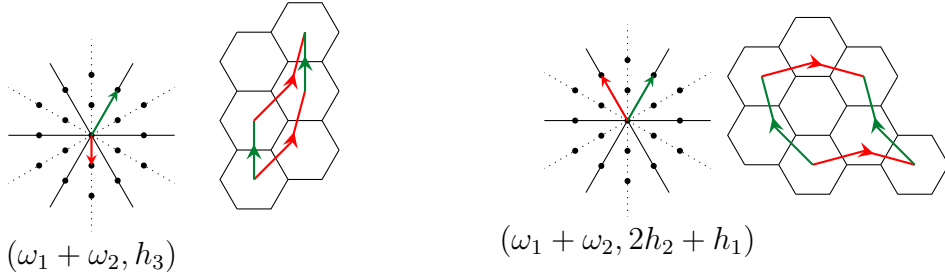


Figure 9: Some more examples of the hexagonal tilings and the dyonic charges

In this section we only discussed the A_2 case. It would be interesting to find a general map from the charge of the dyonic loops to the networks for or general $A_{k>2}$ cases.

5 Some examples in the superconformal index

So far we have been studying the properties of the networks of the class S theories. In this section, we would like to study a few concrete manifestations of our analysis when the four-dimensional side is $S^1 \times S^3$, or equivalently, in the setting of the superconformal index.

As has been well established, the superconformal index of a class S theory of type $SU(N)$, defined by a Riemann surface C of genus g with n full punctures, is given by the (zero-area limit of the) (p, q, t) -deformed Yang-Mills theory on the same Riemann surface [5–7]. Here we consider the case $q = t$ where the p dependence automatically drops out, and the superconformal index becomes the standard q -deformed Yang-Mills theory, defined in [19, 20, 44]. In this case, the supercharge defining the superconformal index is compatible with the presence of a half-BPS line wrapping the S^1 direction [25, 45].

Therefore, in this setup, a defect of a class S theory, specified by a network with labels on the Riemann surface C should be realized as a concrete object in the q -deformed Yang-Mills theory, defined by the same network with labels on C . Below, we show that they are just given by the Wilson lines⁸ and the Wilson junctions in the q -deformed Yang-Mills theory. In particular, we compute the superconformal index of the nontrivial line

⁸This statement was independently obtained by W. Peelaers and L. Rastelli.

operator of the T_3 theory, namely the 6d $\mathcal{N}=(2,0)$ theory of type $SU(3)$ compactified on a sphere with three full punctures. Reassuringly, we will find that the result shows an enhancement of the symmetry from $SU(3)^3$ to E_6 , as it should be, since the T_3 theory is the E_6 theory of Minahan and Nemeshcansky.

Below, we will first very briefly review the relation between the superconformal index and the q -deformed Yang-Mills in Sec. 5.1. Then we check that the superconformal index with a Wilson line in the 4d gauge theory is given by the Wilson line in the 2d gauge theory in Sec. 5.2. Finally, we will compute the superconformal index of a network in the T_3 theory in Sec. 5.3. Note that in this section we use the 2d Yang-Mills normalization of the junctions as discussed in Sec. 3.3.2.

5.1 The superconformal indices without lines

Consider the class S theory $S_{g,n}$ for a genus g surface with n full punctures. Its superconformal index is defined as

$$\mathcal{I}_g(a_1, \dots, a_n) = \text{Tr}(-1)^F q^{\Delta - I_3} a_1 \cdots a_n \quad (5.1)$$

where the trace is over the Hilbert space of the system on S^3 or equivalently on the space of the operators, Δ is the scaling dimension, I_3 is the Cartan generator of $SU(2)_R$ symmetry, and $a_i \in SU(N)_i$ is a group element of the flavor symmetry $SU(N)_i$ of the theory associated to the i -th full puncture.

This is known to be given by the following explicit expression:

$$\mathcal{I}_g(a_1, \dots, a_n) = \sum_{\lambda} \frac{\prod_i K(a_i) \chi_{\lambda}(a_i)}{K_0^{2g-2+n} \chi_{\lambda}(q^{\rho})^{2g-2+n}} \quad (5.2)$$

where the sum is over all the irreducible representations λ of $SU(N)$, $\chi_{\lambda}(a)$ is the character of a in the representation λ , q^{ρ} is the element

$$q^{\rho} = \text{diag}(q^{(N-1)/2}, q^{(N-3)/2}, \dots, q^{(1-N)/2}), \quad (5.3)$$

and $K(a)$, K_0 are given by

$$K(a) = \text{PE}\left[\frac{q}{1-q}(N-1 + \sum_{i \neq j} a_i/a_j)\right], \quad K_0 = \text{PE}\left[\frac{q^2 + q^3 + \dots + q^N}{1-q}\right]. \quad (5.4)$$

Here we took a to be diagonal,

$$a = \text{diag}(a_1, \dots, a_N) \in \text{SU}(N), \quad (5.5)$$

and PE is the plethystic exponential, defined by

$$\text{PE}\left[\sum_{n \geq 1} a_n t^n\right]_t = \prod_{n \geq 1} (1 - t^n)^{-a_n}. \quad (5.6)$$

Take two class S theories $S_{g,n}$ and $S_{g',n'}$, pick one full puncture from each, say the last one from $S_{g,n}$ and the first one from $S_{g',n'}$. Let us then couple $SU(N)$ gauge multiplets to the diagonal combination of the $SU(N)$ symmetries carried by the two full punctures thus chosen. The combined system has the superconformal index

$$\begin{aligned} \mathcal{I}_{g,g'}(a_1, \dots, a_{n-1}; b_2, \dots, b_{n'}) \\ = \int [dz]_{\text{Haar}} K(z)^{-2} \mathcal{I}_g(a_1, \dots, a_{n-1}, z) \mathcal{I}_{g'}(z^{-1}, b_1, \dots, b_{n'}) \end{aligned} \quad (5.7)$$

where $[dz]_{\text{Haar}}$ is the natural measure on the Cartan of $SU(N)$ given by

$$[dz]_{\text{Haar}} = \frac{1}{N!} \prod_{i=1}^{N-1} \frac{dz_i}{2\pi\sqrt{-1}z_i} \prod_{i \neq j} (1 - z_i/z_j). \quad (5.8)$$

Plugging in the expression (5.2) to (5.7) and using the orthogonality of characters

$$\int [dz]_{\text{Haar}} \chi_\lambda(z) \chi_\mu(z^{-1}) = \delta_{\mu\lambda}, \quad (5.9)$$

we see that the equation (5.7) reduces to (5.2) for the genus $g + g'$ surface and $n + n' - 2$ full punctures. This is as it should be.

When $g = 0$ and $n = 3$, what we have is the T_N theory. For $N = 3$, the symmetry $SU(N)^3$ enhances to E_6 . The decomposition is

$$\mathcal{I}_{T_3}(q, \alpha) = 1 + q\chi_{00000} + q^2(\chi_{00000} + \chi_{00000}) + q^3(\chi_{00000} + \chi_{00100} + \chi_{00000} + 2\chi_{00000} + 2)q^3 + \dots \quad (5.10)$$

where $\alpha = (a, b, c)$ is the fugacity for E_6 flavor symmetry, and $\chi_\lambda = \chi_\lambda(\alpha)$ is the character of E_6 in the irreducible representation with Dynkin label λ .

5.2 4d Wilson Lines

Let us move on to the superconformal index in the presence of a loop operator wrapping S^1 [45, 46]. In this subsection, for simplicity, we only study a loop operator that is just a Wilson line with respect to a 4d gauge group. For class S theories, this covers every operator that is a genuine loop L labeled by a representation R on the Riemann surface (*i.e.* all networks without junctions), since we can always cut the Riemann surface along L to go to a duality frame where that particular loop wraps a tube once.

To compute the superconformal index with a Wilson loop, let us first consider a more general situation. Take a theory X with G flavor symmetry whose superconformal index is $\mathcal{I}_X(a)$. Suppose we can couple it with the G vector multiplet, such that the gauge coupling is exactly marginal. Let us insert a BPS Wilson line in the representation R of G . The resulting index is simply

$$\mathcal{I}_R(q) = \int [dz]_{\text{Haar}} K(z)^{-2} \chi_R(z) \mathcal{I}_X(z). \quad (5.11)$$

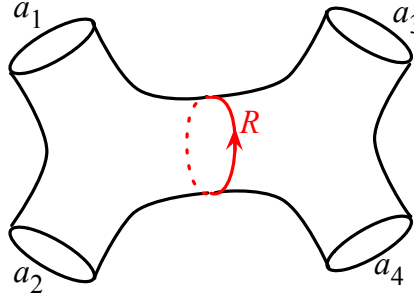


Figure 10: Wilson line around a tube corresponding to a gauge group.

This reduces to the formula (5.7) when R is a trivial representation, as it should be.

Now consider the case when X consists of two copies of the T_N theory, such that we gauge a diagonal combination of G symmetries. We have

$$\begin{aligned} \mathcal{I}_R(q) &= \int [dz]_{\text{Haar}} \frac{K(a_1)K(a_2)K(z)}{K_0} \left[\sum_{\lambda} \frac{\chi_{\lambda}(a_1)\chi_{\lambda}(a_2)\chi_{\lambda}(z)}{\chi_{\lambda}(q^{\rho})} \right] \chi_R(z) \\ &\quad \times K(z)^{-2} \frac{K(z^{-1})K(a_3)K(a_4)}{K_0} \left[\sum_{\lambda'} \frac{\chi_{\lambda'}(z^{-1})\chi_{\lambda'}(a_3)\chi_{\lambda'}(a_4)}{\chi_{\lambda'}(q^{\rho})} \right] \end{aligned} \quad (5.12)$$

$$= \frac{K(a_1)K(a_2)K(a_3)K(a_4)}{K_0^2} \left[\sum_{\lambda, \lambda'} \frac{\chi_{\lambda}(a_1)\chi_{\lambda}(a_2)n_{\lambda R}^{\lambda'}\chi_{\lambda'}(a_3)\chi_{\lambda'}(a_4)}{\chi_{\lambda}(q^{\rho})\chi_{\lambda'}(q^{\rho})} \right] \quad (5.13)$$

where

$$n_{\lambda R}^{\lambda'} = \int [da]_{\text{Haar}} \chi_R(a)\chi_{\lambda}(a)\chi_{\lambda'}(a^{-1}) \quad (5.14)$$

counts how many times the irreducible representation λ' appear in the tensor product $\lambda \otimes R$.

The result (5.13) is, up to the prefactor involving K , the unnormalized correlator of the q -deformed Yang-Mills theory with the Wilson line with the representation R , around the tube associated to the gauge group, see Fig. 10. There, we displayed full punctures as boundaries, as would be more common in the 2d Yang-Mills viewpoint.

For non-deformed 2d Yang-Mills theory, this is an immediate consequence from the fact that the Hilbert space of the system on S^1 is the space of class functions on G , that is spanned by $\chi_{\lambda}(z)$, and the Wilson loop in the representation R acts by a multiplication by $\chi_R(z)$ almost by definition. For q -deformed 2d Yang-Mills theory, we need to use the fact that the structure of the tensor product decomposition of the representations of the quantum group G_q is not deformed as long as q is generic.

5.3 A network in the T_3 theory

As an example of the network that is not just a loop, let us consider the T_3 theory and the 2d network shown in Fig. 11.

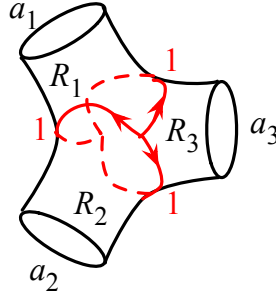


Figure 11: A line operator of T_3 theory, represented as a Wilson junction on the 2d side.

The superconformal index is given by

$$\mathcal{I}_{T_3, \text{network}} = \frac{K(a_1)K(a_2)K(a_3)}{K_0} \sum_{R_1, R_2, R_3} c_{R_1, R_2, R_3} \chi_{R_1}(a_1) \chi_{R_2}(a_2) \chi_{R_3}(a_3) \quad (5.15)$$

where c_{R_1, R_2, R_3} is the amplitude of the q -deformed Yang-Mills, coupling three states $\chi_{R_i}(a_i)$ ($i = 1, 2, 3$) on the three boundaries.

In the undeformed 2d Yang-Mills theory, c_{R_1, R_2, R_3} is given by the integral

$$c_{R_1, R_2, R_3} = \int [dU_1][dU_2][dU_3] \chi_{R_1}(U_2 U_3^{-1}) \chi_{R_2}(U_3 U_1^{-1}) \chi_{R_3}(U_1 U_2^{-1}) \times \epsilon_{ijk} \epsilon^{\bar{i}\bar{j}\bar{k}} (U_1)_{\bar{i}}^i (U_2)_{\bar{j}}^j (U_3)_{\bar{k}}^k, \quad (5.16)$$

where $U_{1,2,3}$ are holonomies of the 2d gauge field from one junction point to the other junction point, along three different segments.

In the q -deformed Yang-Mills theory, we need to perform the integral above in the sense of the quantum group [19, 20]. The U_3 integral gives a nonzero result only when R_1 is contained in $R_2 \otimes V$, where V is the standard three-dimensional representation of $SU(3)_q$. Since the rules of irreducible decompositions of tensor products are unchanged under the q deformation, we see that c_{R_1, R_2, R_3} is nonzero only when the highest weight of R_1 is given by adding to the highest weight of R_2 one of the three weights of V . This means that there is an arrow connecting $R_1 \rightarrow R_2$ in the diagram of irreducible representations as shown in Fig. 12. We immediately see that there we should have arrows similarly for $R_2 \rightarrow R_3$ and $R_3 \rightarrow R_1$. Therefore c_{R_1, R_2, R_3} is nonzero only when $R_1 \rightarrow R_2 \rightarrow R_3 \rightarrow R_1$ forms a triangle in Fig. 12.

Next, consider what happens when the holonomy at a puncture a_3 is set to the special value $a_3 = q^\rho = (q, 1, q^{-1})$. This is equivalent to the absence of the puncture, and we have the situation in Fig. 13. Using the skein relation, we see that the left hand side and the right hand side should be proportional by a factor of [2]. The right hand side is just $\sum_{R_1 \rightarrow R_2} \chi_{R_1}(a_1) \chi_{R_2}(a_2)$. Therefore, c_{R_1, R_2, R_3} is determined by an overconstrained set of equations

$$\sum_{R_2 \rightarrow R_3 \rightarrow R_1 \rightarrow R_2} c_{R_1, R_2, R_3} \chi_{R_3}(q^\rho) = [2]_q \delta_{R_1 \rightarrow R_2} \quad (5.17)$$

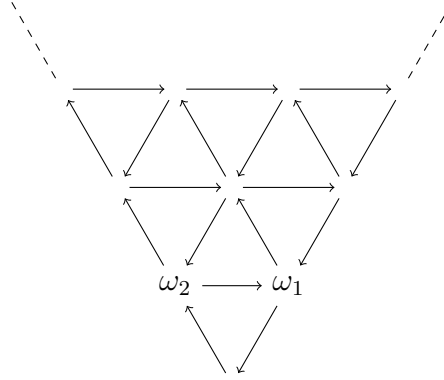


Figure 12: An arrow $R \rightarrow R'$ connects two highest weights R, R' of $SU(3)$ if $R' \otimes V$ contains R . c_{R_1, R_2, R_3} is nonzero only when the arrows form a triangle $R_1 \rightarrow R_2 \rightarrow R_3 \rightarrow R_1$.

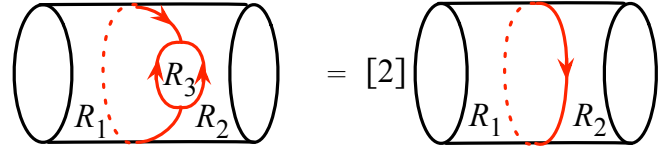


Figure 13: A trick

where the sum on the right hand side is over R_3 that fit in the triangle. This equation can be recursively solved starting from the triangle closest to the origin. We can check that the following gives the general solution⁹:

$$\dim_q(n\omega_1 + m\omega_2) = \chi_{n\omega_1 + m\omega_2}(q^\rho) = \frac{[n+1][m+1][n+m+2]}{[2]}, \quad (5.18)$$

$$c \begin{array}{c} \swarrow n\omega_1 + m\omega_2 \swarrow \\ (n-1)\omega_1 + m\omega_2 \rightarrow n\omega_1 + (m-1)\omega_2 \end{array} = \frac{[2]}{[n+1][m+1][n+m+1]}, \quad (5.19)$$

$$c \begin{array}{c} \nwarrow n\omega_1 + (m+1)\omega_2 \nwarrow \\ n\omega_1 + m\omega_2 \end{array} = \frac{[2]}{[n+1][m+1][n+m+3]}. \quad (5.20)$$

Plugging them into (5.15), we find it nicely becomes a sum of representations of E_6 :

$$\begin{aligned} \mathcal{I}_{T_3, \text{Line}}(q, \alpha) &= q^{1/2} \chi_{10000}^0 + q^{3/2} (\chi_{10000}^1) \\ &\quad + q^{5/2} (\chi_{10000}^0 + \chi_{00010}^0 + \chi_{10000}^1 + \chi_{10000}^2) + \dots \end{aligned} \quad (5.21)$$

⁹The authors thank the twitter user @LT_shu for kindly providing this general solution in https://twitter.com/LT_shu/status/349136595632390144.

Acknowledgments The authors would like to thank Dongmin Gang, Takuya Okuda and Masahito Yamazaki for helpful discussions. YT's work is supported in part by JSPS Grant-in-Aid for Scientific Research No. 25870159. NW is supported by the Advanced Leading Graduate Course for Photon Science, one of the Program for Leading Graduate Schools lead by Japan Society for the Promotion of Science, MEXT, and YT are also supported in part by WPI Initiative, MEXT, Japan at IPMU, the University of Tokyo.

A Examples of OPE and charge/network dictionary

Here we present some more examples of the OPE and the correspondence of the dyonic charge and the networks for the $\mathcal{N}=4$ theory, or equivalently for the torus. The results of the OPE are for $A_{N-1>2}$ unless otherwise stated. For the A_2 case, the edges with 3 should be removed and those with 2 can be replaced by the reversed ones with 1. We use the convention that the magnetic weight lies in the fundamental Weyl chamber Λ/\mathcal{W} but the electric one is unrestricted.

A.1 Pure dyonic loops

Dyonic loops can be roughly classified into two, which we call pure and complex. The pure ones are those that can be mapped to a Wilson loop in a duality frame, and the complex ones are those without any such duality frame. Let us first discuss the representation of the pure ones as loops on the torus.

We abbreviate a bundle of arrows with charges s_1, s_2, \dots, s_{r-1} and s_r as a single arrow without any label:

$$\uparrow := \begin{array}{c} s_1 \ s_2 \ s_3 \dots s_{r-1} \ s_r \\ \uparrow \uparrow \uparrow \dots \uparrow \uparrow \end{array} . \quad (\text{A.1})$$

Let $\omega_I = \sum_{i=1}^r \omega_{s_i}$. Then there are four types as follows:

$$\begin{array}{ll} (\mu_m, \lambda_e) = (p\omega_I, q\omega_I), & (\mu_m, \lambda_e) = (p\omega_I, -q\omega_I) \\ q \geq p : \quad \begin{array}{c} p \\ \overbrace{\quad \quad \quad}^q \end{array} , & \quad \begin{array}{c} p \\ \overbrace{\quad \quad \quad}^q \end{array} , \end{array} \quad (\text{A.2})$$

$$p \geq q : \quad \begin{array}{c} \text{Diagram of } p \text{ strands in a box, } q \text{ strands out.} \end{array} \quad , \quad \begin{array}{c} \text{Diagram of } p \text{ strands in a box, } q \text{ strands out.} \end{array} \quad , \quad (\text{A.3})$$

This is essentially the same as the discussion in [8].

A.2 $W_{\square} \times T_{\square}$

Let us compute the skein relation of W_{\square} and T_{\square} . Comparing with what we expect from the gauge theory, we can then identify various networks with complex dyonic loops. From the skein relation, we have

$$\begin{array}{c} \square \\ \square \end{array} = q^{2/N} \left[\begin{array}{c} \text{Diagram with red horizontal line, green vertical line, blue '2' labels} \\ - \\ \text{Diagram with red diagonal line, blue '2' and '3' labels} \\ + q^{-1} \text{Diagram with blue '2' labels} \\ + q^{-2} \text{Diagram with black lines} \end{array} \right] \quad (\text{A.4})$$

The first term is a new one, the second and third ones are elementary and the final one is pure. Then we identify:

$$D_{[(\omega_1, 2h_{i(\neq 1)})]} \sim \begin{array}{c} \text{Diagram with red diagonal line, blue '2' labels} \end{array} , \quad D_{[(\omega_1, h_{i(\neq 1)} + h_{j(>i)})]} \sim \begin{array}{c} \text{Diagram with red diagonal line, blue '2' and '3' labels} \end{array} , \quad (\text{A.5})$$

$$D_{[(\omega_1, h_1 + h_{i(\neq 1)})]} \sim \begin{array}{c} \text{Diagram with blue '2' labels} \end{array} , \quad D_{[(\omega_1, 2\omega_1)]} \sim \begin{array}{c} \text{Diagram with black lines} \end{array} . \quad (\text{A.6})$$

A.3 $W_{(2,1)} \times T_{\square}$

Let us next consider $W_{(2,1)} \times T_{\square}$:

$$\begin{array}{c}
\boxed{\square} \\
\boxed{\square} \quad = \quad q^{3/N} \left[\begin{array}{c} \text{Diagram 1: } \text{Red horizontal line, green vertical line, blue numbers 2, 3, 2, 2} \\ \text{Diagram 2: } \text{Red horizontal line, green vertical line, blue numbers 2, 3, 2, 2} \\ \text{Diagram 3: } \text{Red diagonal line, green diagonal line, blue numbers 3, 4, 3} \\ \text{Diagram 4: } \text{Red horizontal line, green horizontal line, blue numbers 2, 2, 2} \\ \text{Diagram 5: } \text{Red diagonal line, green diagonal line, blue numbers 2, 2, 2} \end{array} \right] \quad (A.7)
\end{array}$$

The first and the third terms are new, the second one is elementary and the fourth one is obtained by a T action of some elementary one. When $N = 3$, the second one does not appear and indeed this case is the same as Example A.5.

We can therefore identify:

$$\begin{array}{c}
D_{[(\omega_1, 2h_{i(\neq 1)} + h_{j(>i)})]} \sim \text{Diagram 1} , \quad D_{[(\omega_1, h_{i(\neq 1)} + h_{j(>i)} + h_{k(>j)})]} \sim \text{Diagram 3} , \quad (A.8) \\
D_{[(\omega_1, h_1 + 2h_{i(\neq 1)})]} \sim \text{Diagram 4} , \quad D_{[(\omega_1, 2h_1 + h_{i(\neq 1)})]} \sim \text{Diagram 5} . \quad (A.9)
\end{array}$$

A.4 $W_{\square\square} \times T_{\square}$

Our next example is $W_{\square\square} \times T_{\square}$:

$$\begin{array}{c}
\boxed{\square} \\
\boxed{\square\square} \quad = \quad q^{3/N} \left[\begin{array}{c} \text{Diagram 1: } \text{Red horizontal line, green vertical line, blue numbers 2, 2, 2, 2} \\ \text{Diagram 2: } \text{Red diagonal line, green diagonal line, blue numbers 3, 4, 3} \end{array} \right] \\
- 2 \quad + \quad
\end{array}$$

$$\begin{aligned}
& + q^{-1} \left(\begin{array}{c} \text{Diagram 1} \\ \text{Diagram 2} \end{array} - \begin{array}{c} \text{Diagram 3} \\ \text{Diagram 4} \end{array} \right) \\
& + q^{-2} \begin{array}{c} \text{Diagram 5} \end{array} + q^{-3} \begin{array}{c} \text{Diagram 6} \end{array} \quad \Big] \quad (\text{A.10})
\end{aligned}$$

The first term is new, the fifth one is elementary, the seventh one is pure and others have appeared in the previous case. When $N = 3$, the third one does not appear. We therefore identify:

$$D_{[(\omega_1, 3h_{i(\neq 1)})]} \sim \begin{array}{c} \text{Diagram 7} \end{array}, \quad D_{[(\omega_1, h_1 + h_{i(\neq 1)} + h_{j(>i)})]} \sim \begin{array}{c} \text{Diagram 8} \end{array}, \quad (\text{A.11})$$

$$D_{[(\omega_1, 3\omega_1)]} \sim \begin{array}{c} \text{Diagram 9} \end{array}. \quad (\text{A.12})$$

A.5 $W_{\text{Adj}} \times T_{\square}$

As a further example, let us consider $W_{\text{Adj}} \times T_{\square}$:

$$\begin{array}{c} \square \\ \text{Diagram 10} \end{array} \text{Adj} = \begin{array}{c} \text{Diagram 11} \\ + \end{array} \begin{array}{c} \text{Diagram 12} \\ + \end{array} \begin{array}{c} \text{Diagram 13} \\ + \end{array} \quad (\text{A.13})$$

The second term is new, and the first and the third ones are obtained by some duality actions of some elementary one. Our identifications are:

$$D_{[(\omega_1, h_{i(\neq 1)} - h_1)]} \sim \text{Diagram 1}, \quad D_{[(\omega_1, h_{i(\neq 1)} - h_{j(\neq i)} + h_{j(>i)})]} \sim \text{Diagram 2}, \quad (\text{A.14})$$

$$D_{[(\omega_1, h_1 - h_{i(\neq 1)})]} \sim \text{Diagram 3}. \quad (\text{A.15})$$

A.6 $W_{\text{Adj}} \times T_{\text{Adj}}$

We now move on to the example $W_{\text{Adj}} \times T_{\text{Adj}}$:

$$\begin{aligned} \text{Adj} &= \text{Diagram 4} + \text{Diagram 5} + \text{Diagram 6} \\ &+ q^{-2} \text{Diagram 7} + q^2 \text{Diagram 8} \\ &+ (2[N-2] + [N-4]) \text{Diagram 9} + (3 + q^2 + q^{-2}) \text{Diagram 10} \\ &+ q^{-1} \left(\text{Diagram 11} + \text{Diagram 12} \right) \\ &+ q \left(\text{Diagram 13} + \text{Diagram 14} \right) \quad (\text{A.16}) \end{aligned}$$

The first one does not appear when $N = 3$ but reduces to a sum of simpler ones.

Then the charge/network dictionary for the new ones is:

$$D_{[(\lambda_{\text{Adj}}, h_{i(\neq 1, N)} - h_1)]} \sim \begin{array}{c} \text{Diagram with 2 loops and 4 nodes labeled 2} \end{array}, \quad (\text{A.17})$$

$$D_{[(\lambda_{\text{Adj}}, h_{i(\neq 1)} - h_N)]} \sim \begin{array}{c} \text{Diagram with 2 loops and 4 nodes labeled 2} \end{array}, \quad D_{[(\lambda_{\text{Adj}}, h_1 - h_{i(\neq 1, N)})]} \sim \begin{array}{c} \text{Diagram with 2 loops and 4 nodes labeled 2} \end{array}, \quad (\text{A.18})$$

$$D_{[(\lambda_{\text{Adj}}, -h_1 + h_{i(\neq 1, N)})]} \sim \begin{array}{c} \text{Diagram with 2 loops and 4 nodes labeled 2} \end{array}, \quad D_{[(\lambda_{\text{Adj}}, h_N - h_{i(\neq 1, N)})]} \sim \begin{array}{c} \text{Diagram with 2 loops and 4 nodes labeled 2} \end{array} \quad (\text{A.19})$$

where $\lambda_{\text{Adj}} = h_1 - h_N$ is the highest weight of the adjoint representation.

A.7 An OPE of complex dyonic loops

Finally we give an example of the OPE of two elementary dyonic loops $D_{(0)}^{1,1}$ and $D_{(0)}^{\ell,k}$ for $\ell, k \leq N/2$ in $\mathcal{N}=4$ SYM:

$$\begin{array}{c} \text{Diagram with 2 loops and 4 nodes labeled 1, k, \ell, k+\ell} \\ \times \text{Diagram with 2 loops and 4 nodes labeled 1, k, \ell, k+\ell} \end{array} = q^{k-\ell/N} \left[\begin{array}{c} \text{Diagram with 2 loops and 4 nodes labeled 1, k, \ell, k+\ell} \\ + q^{-1} \text{Diagram with 2 loops and 4 nodes labeled 1, k, \ell+2, k+1} \\ + q \text{Diagram with 2 loops and 4 nodes labeled 1, k, \ell, k+2} \end{array} \right] \quad (\text{A.20})$$

where

- the first term corresponds to $D_{[(\omega_\ell + \omega_1, 2h_{j_s=1} + \sum_{s=2}^k h_{j_s})]}$ where $j_s > \ell$,
- the second one to $D_{[(\omega_{\ell+1}, h_{i(\leq \ell+1)} + 2h_{j_s=1} + \sum_{s=2}^{k-1} h_{j_s})]}$ where $j_s > \ell + 1$,

- the third one to $D_{[(\omega_\ell + \omega_1, h_{(1 < i)_{i(\leq \ell)}} + \sum_{s=1}^k h_{j_s})]}$ where $j_s > \ell$.

Here we require j_s differ for each s . It would be interesting to apply the diagrammatic approach to more complicated OPEs and read off the charge information from networks in general.

References

- [1] D. Gaiotto, *$N=2$ dualities*, *JHEP* **1208** (2012) 034, [0904.2715].
- [2] D. Gaiotto, G. W. Moore, and A. Neitzke, *Wall-crossing, Hitchin Systems, and the WKB Approximation*, 0907.3987.
- [3] L. F. Alday, D. Gaiotto, and Y. Tachikawa, *Liouville Correlation Functions from Four-dimensional Gauge Theories*, *Lett.Math.Phys.* **91** (2010) 167–197, [0906.3219].
- [4] N. Wyllard, *$A(N-1)$ conformal Toda field theory correlation functions from conformal $N=2$ $SU(N)$ quiver gauge theories*, *JHEP* **0911** (2009) 002, [0907.2189].
- [5] A. Gadde, E. Pomoni, L. Rastelli, and S. S. Razamat, *S -Duality and 2D Topological QFT*, *JHEP* **1003** (2010) 032, [0910.2225].
- [6] A. Gadde, L. Rastelli, S. S. Razamat, and W. Yan, *The 4D Superconformal Index from Q -Deformed 2D Yang-Mills*, *Phys.Rev.Lett.* **106** (2011) 241602, [1104.3850].
- [7] A. Gadde, L. Rastelli, S. S. Razamat, and W. Yan, *Gauge Theories and Macdonald Polynomials*, *Commun.Math.Phys.* **319** (2013) 147–193, [1110.3740].
- [8] N. Drukker, D. R. Morrison, and T. Okuda, *Loop operators and S -duality from curves on Riemann surfaces*, *JHEP* **0909** (2009) 031, [0907.2593].
- [9] E. P. Verlinde, *Fusion Rules and Modular Transformations in 2D Conformal Field Theory*, *Nucl.Phys.* **B300** (1988) 360.
- [10] L. F. Alday, D. Gaiotto, S. Gukov, Y. Tachikawa, and H. Verlinde, *Loop and surface operators in $N=2$ gauge theory and Liouville modular geometry*, *JHEP* **1001** (2010) 113, [0909.0945].
- [11] N. Drukker, J. Gomis, T. Okuda, and J. Teschner, *Gauge Theory Loop Operators and Liouville Theory*, *JHEP* **1002** (2010) 057, [0909.1105].
- [12] N. Drukker, D. Gaiotto, and J. Gomis, *The Virtue of Defects in 4D Gauge Theories and 2D CFTs*, *JHEP* **1106** (2011) 025, [1003.1112].
- [13] J. Gomis and B. Le Floch, *$'t$ Hooft Operators in Gauge Theory from Toda CFT*, *JHEP* **1111** (2011) 114, [1008.4139].

- [14] D. Xie, *Higher laminations, webs and $N=2$ line operators*, 1304.2390.
- [15] M. Bullimore, *Defect Networks and Supersymmetric Loop Operators*, 1312.5001.
- [16] G. Kuperberg, *Spiders for rank 2 Lie algebras*, *Comm. Math. Phys.* **180** (1996), no. 1 109–151, [[q-alg/9712003](#)].
- [17] H. Murakami, T. Ohtsuki, and S. Yamada, *Homfly polynomial via an invariant of colored plane graphs*, *Enseign. Math. (2)* **44** (1998), no. 3-4 325–360.
- [18] C. Gómez, M. Ruiz-Altaba, and G. Sierra, *Quantum groups in two-dimensional physics*. Cambridge Monographs on Mathematical Physics. Cambridge University Press, Cambridge, 1996.
- [19] A. Y. Alekseev, H. Grosse, and V. Schomerus, *Combinatorial Quantization of the Hamiltonian Chern-Simons Theory*, *Commun.Math.Phys.* **172** (1995) 317–358, [[hep-th/9403066](#)].
- [20] E. Buffenoir and P. Roche, *Two-Dimensional Lattice Gauge Theory Based on a Quantum Group*, *Commun.Math.Phys.* **170** (1995) 669–698, [[hep-th/9405126](#)].
- [21] A. Kapustin, *Wilson-’t Hooft operators in four-dimensional gauge theories and S-duality*, *Phys.Rev.* **D74** (2006) 025005, [[hep-th/0501015](#)].
- [22] J. A. Minahan and D. Nemeschansky, *An $\mathcal{N}=2$ Superconformal Fixed Point with E_6 Global Symmetry*, *Nucl. Phys.* **B482** (1996) 142–152, [[hep-th/9608047](#)].
- [23] S. Gukov and E. Witten, *Gauge Theory, Ramification, and the Geometric Langlands Program*, [hep-th/0612073](#).
- [24] D. Gaiotto, G. W. Moore, and A. Neitzke, *Framed BPS States*, 1006.0146.
- [25] T. Dimofte, D. Gaiotto, and S. Gukov, *3-Manifolds and 3D Indices*, 1112.5179.
- [26] Y. Ito, T. Okuda, and M. Taki, *Line operators on $S^1 \times R^3$ and quantization of the Hitchin moduli space*, *JHEP* **1204** (2012) 010, [[1111.4221](#)].
- [27] T. Okuda, *Line Operators in Supersymmetric Gauge Theories and the 2D-4D Relation*, 1412.7126.
- [28] S. Gukov, *Surface Operators*, 1412.7127.
- [29] N. Hama and K. Hosomichi, *Seiberg-Witten Theories on Ellipsoids*, *JHEP* **1209** (2012) 033, [[1206.6359](#)].
- [30] J. Gomis, T. Okuda, and V. Pestun, *Exact Results for ’t Hooft Loops in Gauge Theories on S^4* , *JHEP* **1205** (2012) 141, [[1105.2568](#)].

- [31] M.-J. Jeong and D. Kim, *The quantum $sl(n, \mathbb{C})$ representation theory and its applications*, *J. Korean Math. Soc.* **49** (2012), no. 5 993–1015, [[math/0506403](#)].
- [32] S. Cautis, J. Kamnitzer, and S. Morrison, *Webs and quantum skew Howe duality*, *Math. Ann.* **360** (2014), no. 1-2 351–390, [[1210.6437](#)].
- [33] A. Chirvasitu and M. Tucker-Simmons, *Remarks on quantum symmetric algebras*, *Journal of Algebra* **397** (2014) 589 – 608, [[1206.1614](#)].
- [34] Y. Tachikawa, *On the 6D Origin of Discrete Additional Data of 4D Gauge Theories*, *JHEP* **1405** (2014) 020, [[1309.0697](#)].
- [35] I. H. Kauffman, *Knots and Physics*, vol. 1 of *Series on Knots and Everything*. World Scientific, 1991.
- [36] E. Witten, *Gauge Theories and Integrable Lattice Models*, *Nucl.Phys.* **B322** (1989) 629.
- [37] V. Pestun, *Localization of gauge theory on a four-sphere and supersymmetric Wilson loops*, *Commun.Math.Phys.* **313** (2012) 71–129, [[0712.2824](#)].
- [38] A. Kapustin and E. Witten, *Electric-Magnetic Duality And The Geometric Langlands Program*, *Commun.Num.Theor.Phys.* **1** (2007) 1–236, [[hep-th/0604151](#)].
- [39] N. Saulina, *A Note on Wilson-’t Hooft Operators*, *Nucl.Phys.* **B857** (2012) 153–171, [[1110.3354](#)].
- [40] R. Moraru and N. Saulina, *OPE of Wilson-’t Hooft operators in $N=4$ and $N=2$ SYM with gauge group $G=PSU(3)$* , [1206.6896](#).
- [41] A. Hanany and K. D. Kennaway, *Dimer Models and Toric Diagrams*, [hep-th/0503149](#).
- [42] S. Franco, A. Hanany, K. D. Kennaway, D. Vegh, and B. Wecht, *Brane Dimers and Quiver Gauge Theories*, *JHEP* **01** (2006) 096, [[hep-th/0504110](#)].
- [43] A. Hanany, D. Orlando, and S. Reffert, *Sublattice Counting and Orbifolds*, *JHEP* **1006** (2010) 051, [[1002.2981](#)].
- [44] M. Aganagic, H. Ooguri, N. Saulina, and C. Vafa, *Black Holes, Q-Deformed 2D Yang-Mills, and Non-Perturbative Topological Strings*, *Nucl.Phys.* **B715** (2005) 304–348, [[hep-th/0411280](#)].
- [45] D. Gang, E. Koh, and K. Lee, *Line Operator Index on $S^1 \times S^3$* , *JHEP* **1205** (2012) 007, [[1201.5539](#)].
- [46] D. Gang, E. Koh, and K. Lee, *Superconformal Index with Duality Domain Wall*, *JHEP* **1210** (2012) 187, [[1205.0069](#)].